DESIGN OF AN EXPERIMENTAL FACILITY FOR THE VALIDATION OF COOLING LOAD CALCULATION PROCEDURES

by

DAVID S. ELDRIDGE, JR.

Bachelor of Science in Mechanical Engineering

University of Illinois

Urbana, IL

1998

Submitted to the Faculty
of the Graduate College of the
Oklahoma State University
in partial fulfillment of
the requirements for
the Degree of
MASTER OF SCIENCE
May, 2007

DESIGN OF AN EXPERIMENTAL FACILITY FOR

THE VALIDATION OF COOLING

LOAD CALCULATION

PROCEDURES

Thesis Approved:

Daniel E. Fisher, P.E.

Thesis Advisor

Jeffrey D. Spitler, P.E.

Afshin J. Ghajar, P.E.

A. Gordon Emslie, Ph.D.

Dean of the Graduate College

Preface and Acknowledgements

I thank everyone for the opportunity to work on the research project that led to this thesis. ASHRAE's new cooling load procedures were an extremely interesting topic. The knowledge gained working to construct the facility to validate the procedures will serve me well professionally, and through life in general. Even in my new professional life the papers generated by this research have generated conversations at local engineering events. I hope that the test facility will live on, not in infamy, but as a useful tool for future research projects in the MAE department.

I would like to thank: Dr. Fisher for helping me get this far and not giving up on me. Deep heartfelt thanks to my parents for sticking by me and helping me through school. I also want to thank Dr. Rees and Dr. Spitler, Chanvit and Calvin, Dustin, Brett, Sam, Sean and the other graduate students. Special thanks for all of the "troubles" I caused to MAE office staff, and thank you to the committee members who have helped me make the last hurdle in the path to my degree. Also thank you to Caryn and my employer, Grumman/Butkus Associates, for understanding my desire to finish this project even after working in the "real" world for several years.

Thank you also to ASHRAE Technical Committee 4.1, *Load Calculations*, and especially Tom and Steve who helped guide the project to a successful conclusion. The project would not have existed without ASHRAE's technical and financial support.

Table of Contents

Table of Figures

Table of Tables

Chapter 1

Introduction

One of the first steps in building thermal analysis usually begins with the calculation of the "cooling load" associated with each of the building's thermal zones. System and equipment sizing are derived from the cooling load. As such, the accuracy of the algorithm for cooling load determination will have a great effect on the future comfort of building inhabitants, the building energy efficiency and the cost to construct the HVAC systems.

The cooling load is the rate of heat removal required to maintain a space at a fixed temperature. This is the goal of the HVAC design engineer – to provide a comfortable indoor environment to match the usage of the building, be it by control of temperature, humidity, or other factors. Space temperature must be specified for a cooling load to have any useful meaning. Decrease the setpoint temperature and the cooling load will increase for a given zone configuration and heat gain profile.

Given a space with specified heat transfer surfaces, gains and HVAC parameters the cooling loads can be calculated. Many different algorithms exist to perform these calculations based on the component heat gains. In order for the methods to be embraced by the design community they must be shown to produce accurate results. The A/E

design office, by its nature, must use procedures that are guaranteed to meet the needs of its clients.

The objective of this investigation is to develop and test an experimental facility with which the new ASHRAE cooling load procedures can be validated. The facility will be used to validate the overall procedure and, whenever possible, to investigate the performance of constituent models.

Cooling loads themselves are well understood in regard to what causes them and generally what magnitude they are. Due to the very complicated heat transfer involved, the exact value of a cooling load may only be known once the zones are constructed. Architects and engineers have been using various methods to predict what these ultimate cooling loads would be for many years, trading off accuracy and usability to varying degrees. These methods have always consistently over-predicted the actual cooling load as long as the correct inputs were used. A number of early procedures exist that vary in their accuracy, practicality and level of over-prediction. These processes have seen major advances in the past thirty years.

In 1997 ASHRAE completed two new cooling load calculation procedures in order to improve accuracy and usability for the cooling load calculation process. The new methods, the Heat Balance Method (Pedersen 1997) and the Radiant Time Series Method (Spitler, Fisher, Pedersen 1997) had little experimental data to back them up. This

project designed and constructed a facility specifically to test these methods and their component models. The table below is a map for this thesis:

Chapter 1	Introduction to the research project
Chapter 2	Description of the cooling load calculation procedures
Chapter 3	Design criteria for the experimental facility and explanation of the design features relative to the aspects of the procedures to tested.
Chapter 4	Instrumentation and controls for the HVAC system and measurement of the experimental data.
Chapter 5	Explanation of the procedure for performing experimental validation testing.
Chapter 6	Experimental facility validation.
Chapter 7	Experimental uncertainty analysis for validation experiments.
Chapter 8	Facility operation and performance
Chapter 9	Conclusions and recommendations for the experimental facility design.

Two general notes for this thesis. First, the subject methods to be validated deal with the zone cooling loads. Air-handling system design is outside the scope of this project. The air system design included as part of this project was developed strictly to accomplish the measurement goals and does not translate to HVAC design practice – in contrast to the space cooling load calculation procedures which are expected to see widespread usage by the design community. Second, the units presented are generally in English units which reflect the common practices in industry. Some of the component models are developed

only in SI units, these models may be presented with SI units in the text to remain consistent with common practice. Software that is used to perform the procedures (whether application or spreadsheet based) will have the capabilities to provide input and output in either system of units.

Chapter 2

Description of the Cooling Load Calculation Procedures

Chapter 2 provides a brief overview of some of the cooling load calculation procedures beginning with the early ASHRAE methods and continuing with the new methods that were the motivation for this research.

2.1 Early ASHRAE Methods

Early cooling load calculation methods, including CLTD/CLF and TETD/TA, were hand calculations, able to be performed using a few table lookups with pencil and paper. These methods attempted to boil down the transient effect of the combined heat transfer processes to simple correlation factors that could be applied to steady state results. These methods required experience and judgment to be used successfully. The TETD/TA procedure, appearing in the 1967 Handbook of Fundamentals (ASHRAE 1967), required the user to choose lag and decrement factors from tables in order to approximate the conversion of radiant heat into a cooling load. Although the results of the procedure were generally found to be adequate, choosing the proper factors required experience. The CLTD/CLF procedure was perhaps the easiest method to use. However, it relied on CLTD factors that were derived from the results of another early method. For cases where the building being designed matched one of the cases used to develop the CLTD factors, the results would be quite reasonable. Many times in practice however the design case might lie somewhere between tested cases – or even worse, outside of the range of

parameters used to develop the CLTD factors. ASHRAE realized that to develop a sufficiently large set of available factors the data set would become unmanageable.

Another early ASHRAE load calculation method was the transfer function method, which was documented as to its usage by McQuiston and Spitler (McQuiston and Spitler 1992). The TFM had been in existence for some time with the method used as the basis to generate factors for the other simplified methods or used alone as one of the most accurate methods of its day. The TFM utilized conduction transfer functions to solve the transient problem. The TFM required an iterative solution scheme, which made it difficult for hand calculations. McQuiston and Spitler included computer programs that could be used to look-up the necessary factors for the TFM as well as the earlier methods, so that the TFM could be more easily used directly.

The practical result was that for non-standard cases the designer would have to use the TFM one way or the other – either to find the solution, or to develop the factors necessary to solve the solution by CLTD. McQuiston and Spitler provided an introduction to performing these methods on a DOS based computer system which simplified the process, one of the hurdles to implementation of the TFM in engineering practice.

2.2 New ASHRAE Procedures

2.2.1 Motivation for Developing New Procedures

Many states and municipalities are enacting energy standards, or adopting existing codes such as the International Energy Conservation Code (IECC) or ASHRAE Standard 90.1

(ASHRAE 2004) in order to mandate energy conservation. This has reset the bar for energy efficiency in building design. Several of the requirements of the code regarding energy streams prescriptively require fan or pumping system efficiency. These efficiencies will better meet the intent of the standard if the system sizing calculations are based on more accurate load calculations.

In addition to motivation for energy efficiency, many organizations are using life-cycle cost analysis to determine which mechanical systems will be installed in their facilities. Oversizing of mechanical systems can lead to increased first costs for equipment, pumps, piping, etc. Optimally sized equipment then immediately reduces construction costs and improves efficiencies for the owner during the long-term.

Electric utility deregulation also has exposed many areas of the United States to higher energy prices, resulting in increased demands from building owners to specify energy efficient HVAC systems.

Regulatory issues and cost pressures aside, the ASHRAE cooling load calculation procedures have been under constant improvement through the years as the membership strived to achieve the best possible balance between accuracy and usability. The usability hurdles have been lowered due to the recent improvements in personal computer technology while the accuracy goal has remained high throughout.

The Heat Balance Method is not strictly speaking a “new” method - it has been around for years. Many of the prior methods have the Heat Balance Method as their origin, having been developed as simplified implementations of the more rigorous Heat Balance Method. In the consulting world it was primarily used in energy simulation applications as opposed to design load calculations. The detailed inputs and hourly solution methods are not suitable for a hand calculation. ASHRAE TC 4.1 sponsored this research to validate both the heat balance algorithm and a simplified version of the Heat Balance Method called the Radiant Time Series Method that is capable of being performed on a spreadsheet.

As mentioned before, due to advances in computing technology over the past two decades it is now practical to run a Heat Balance Method calculation in a design office. The Radiant Time Series Method follows along as a method based on the fundamental Heat Balance Method while facilitating forensic analysis of the load components, such as the heat gain through the roof or floor. Additionally the Radiant Time Series Method is suitable for use in a spreadsheet application, which aids both the design professional as well as serving in a pedagogical sense. Almost every design office and consulting firm will have spreadsheet software at every engineer’s workstation. Students of the science will benefit from being able to see the different load components developed as part of the solution process instead of just the end result in the full Heat Balance Method.

ASHRAE’s next step towards the widespread implementation of these methods is to provide data documenting their accuracy. Since the methods include many

simplifications, it is not expected that the methods will match exactly for 100% of the cases. The test facility must therefore be designed to both validate a wide range of cooling load conditions as well as provide detailed component information that will support analysis and extension of the subordinate models.

2.2.2 Heat Balance Method

The Heat Balance Method is based upon the 1st Law of Thermodynamics applied to three control volumes, and is shown graphically in Figure 2-1 (Pedersen, Fisher, Liesen 1997). The three control volumes encompass the exterior surfaces, the interior surfaces and the zone air mass.

The exterior heat balance is defined by a control volume at the interface between the outside surface and environment. Direct solar radiation, diffuse solar radiation, longwave radiation exchange with the environment and convection all enter the control volume through the exterior surface. Conduction to the interior of the construction leaves the other surface. (Note that heat flow may be positive or negative for conduction, radiation exchange with the environment or convection depending on conditions, however diffuse and solar radiation will always be into the surface or zero.) This process is repeated for each surface, as indicated in Figure 2-1.

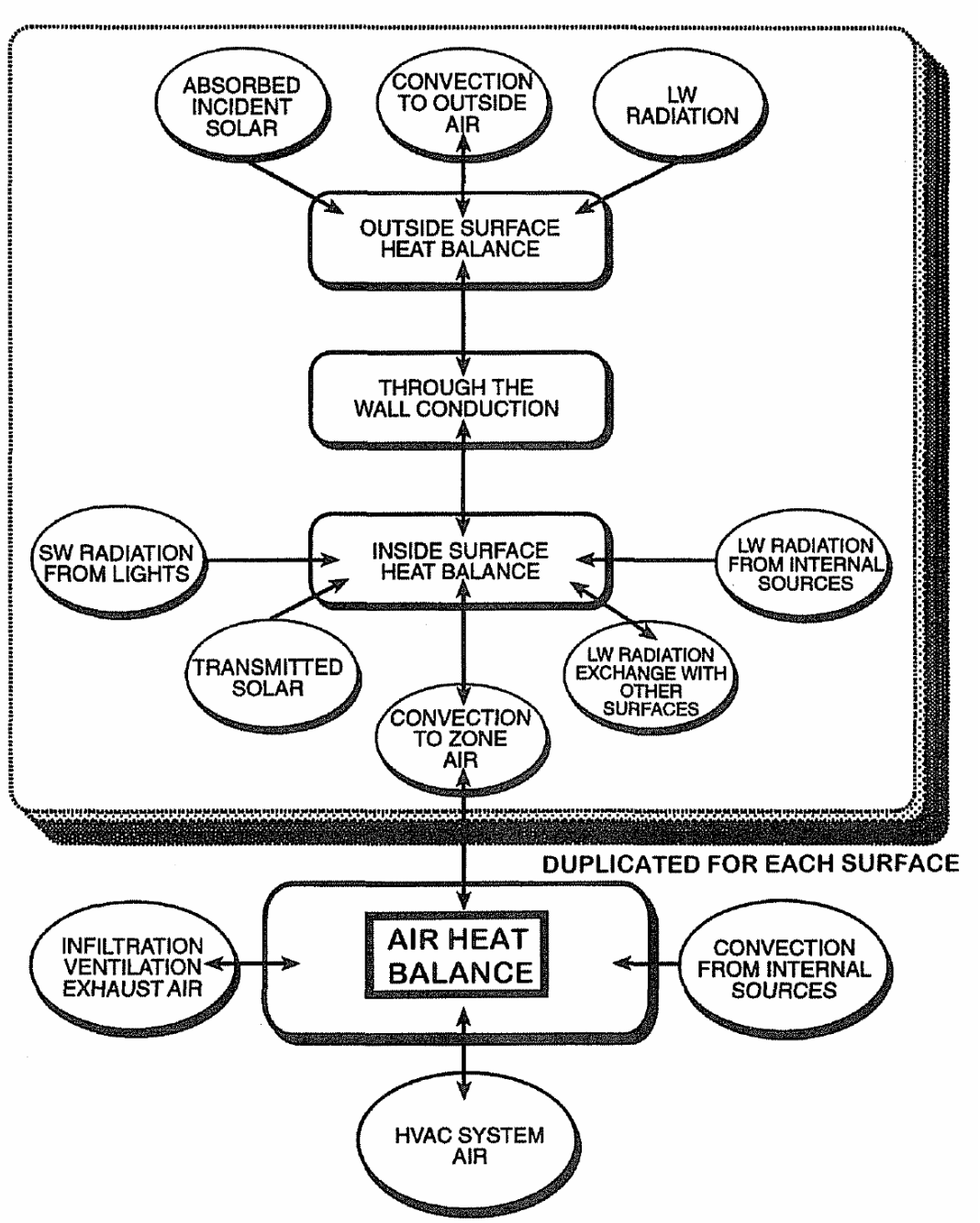

Figure 2-1 Graphical depiction of the Heat Balance Method from Pedersen (1997)

The second heat balance is at the interior surface of the construction. A control volume is taken around the inner surface where conduction, convection, radiation exchange with the other interior surfaces, radiation from other sources, and transmitted solar all enter or

leave the control volume. The interior heat balance is linked to the exterior heat balance by conduction and the thermal storage in the wall construction. Similar to the exterior heat balance, the interior heat balance is repeated for each surface.

The third heat balance is based on a control volume that includes only the mass of air in the zone. Convection transfers heat from the zone surfaces to the control volume, air infiltration transfers heat directly from the outside environment, internal sources may contribute energy through convection and the mechanical system extracts heat from the control volume. The processes interacting directly with the air heat balance are solved only once for each zone.

The heat balance equations from Pedersen are shown below.

Exterior Heat Balance

$$q''_{\alpha sol} + q''_{LWR} + q''_{conv} = q''_{k,o} \quad \textbf{(2-1)}$$

Where:

$q''_{\alpha sol}$	=	absorbed direct and diffuse solar radiation heat flux (shortwave)	Btu/(hr·ft^2)
q''_{LWR}	=	net longwave radiation absorbed from the surroundings	Btu/(hr·ft^2)
q''_{conv}	=	convective flux from the outside air	Btu/(hr·ft^2)
$q''_{k,o}$	=	conductive heat flux into the wall surface (shown positive for heat flux from the exterior to the interior)	Btu/(hr·ft^2)

Interior Heat Balance

$$q''_{k,i} + q''_{solar} = q''_{conv} + q''_{LWRexch} + q''_{SWR} + q''_{equipR} \quad \textbf{(2-2)}$$

where:

q''_{conv}	=	convective heat flux to the zone air	Btu/(hr·ft^2)
$q''_{LWRexch}$	=	net longwave radiation emitted by zone surface	Btu/(hr·ft^2)
q''_{sol}	=	transmitted solar radiation absorbed by zone surface	Btu/(hr·ft^2)
$q''_{k,i}$	=	conduction at the inner surface, shown positive into the control volume	Btu/(hr·ft^2)
q''_{equipR}	=	radiation from equipment and other internal sources in the zone	Btu/(hr·ft^2)
q''_{SWR}	=	shortwave radiation from lights	Btu/(hr·ft^2)

Air Heat Balance

$$q''_{conv} + q_{CE} + q_{IV} + q''_{sys} = 0 \quad \textbf{(2-3)}$$

where:

q''_{conv}	=	convective heat transfer from surfaces	Btu/(hr·ft^2)
q''_{CE}	=	convection from internal sources (equipment)	Btu/(hr·ft^2)
q''_{IV}	=	heat transfer from infiltration and ventilation	Btu/(hr·ft^2)
q''_{sys}	=	heat transfer to the HVAC system	Btu/(hr·ft^2)

In the Heat Balance Method, these equations would be solved iteratively starting with the inside and outside surface temperatures of each surface. Typically, conduction transfer

functions (CTF's) are used to solve the transient conduction linking the outside and inside heat balances.

The air heat balance is solved for q''_{sys} which is the system "heat extraction rate" in a cooling load calculation. Once the successive substitution procedure has converged, the extraction rate for a constant zone setpoint is defined as the cooling load.

2.2.3 Radiant Time Series Method

The Radiant Time Series Method (RTSM) was developed in order to provide a simplified version of the Heat Balance Method that would be suitable for implementation in a spreadsheet. Another intended benefit of the method is that the radiant time series terms provide insight into the dominant building heat transfer processes.

The RTSM begins with the calculation of exterior boundary conditions as shown in Figure 2-2. These must be calculated outside of the procedure. Heat gains are then calculated and split into radiative and convective portions. Zone response factors called "Radiant Time Factors" are used to convert the radiative portion of the gains into a portion of the cooling load. The remainder of the cooling load comes from the convective heat gains which are assumed to occur instantaneously.

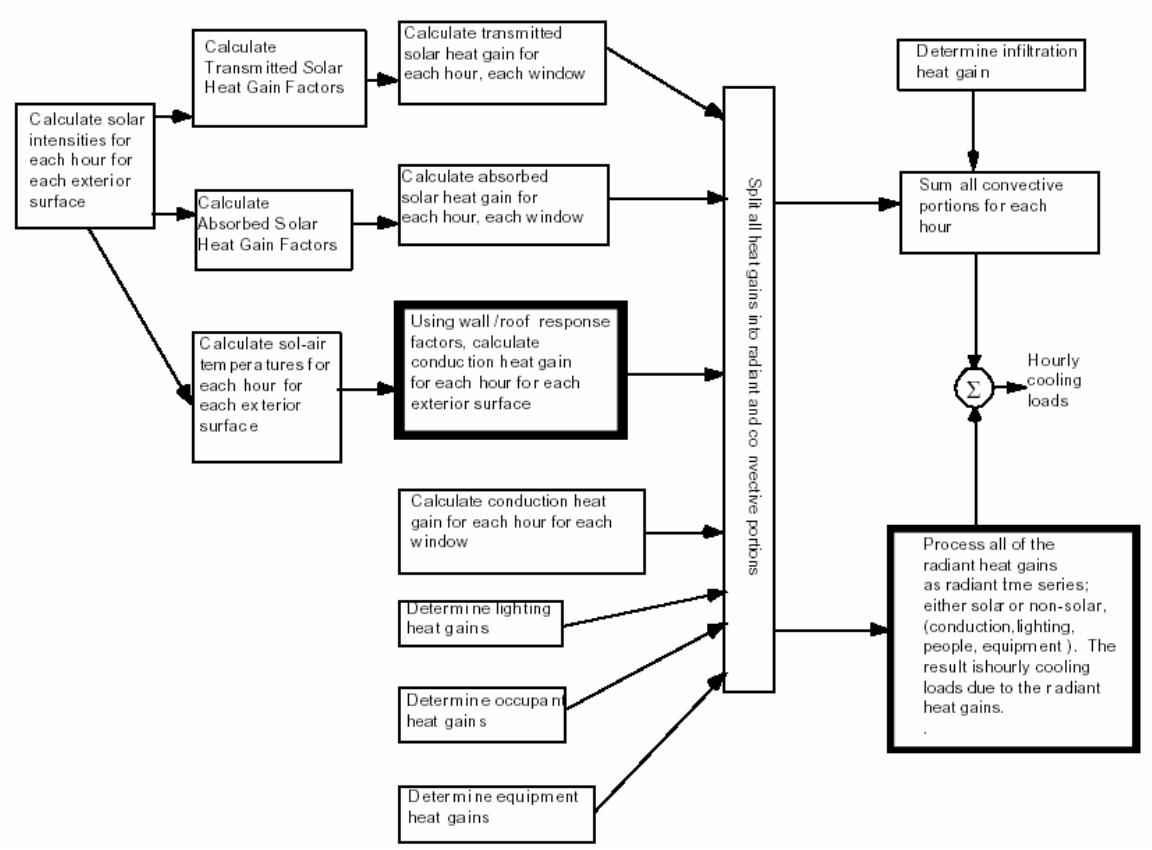

Figure 2-2 Radiant Time Series Method flowchart (Spitler, Fisher, Pedersen 1997)

The RTSM makes several assumptions in order to calculate the cooling load with such a simple formulation:

- There is no exterior heat balance in the RTSM. Instead, an equivalent temperature is used to approximate the heat transfer that would have occurred from exterior convection, radiation exchange and solar radiation.
- Periodic response factors replace the conduction transfer functions.
- Instead of an interior heat balance, the convection coefficient is included as an additional thermal resistance in the conduction calculation. The conduction heat gain is split into convective and radiative portions.
- Instead of a zone air heat balance, the cooling load is a direct product of the method and is calculated by summing the convective gains and converting the radiant gains to cooling loads by means of radiant time factors. The radiant time factors approximate the transient conduction calculation and the thermal storage effect.
- Steady periodic boundary conditions are assumed in the calculation of the periodic response factors and the radiant time factors.

These assumptions result in several limitations to the method as a whole. The storage and release of energy are now prescribed by fixed factors and will not be affected by surface temperatures. There are also limitations imposed by the need to pre-calculate response factors and radiant time factor libraries for simple spreadsheet applications. Note that the Heat Balance Method will calculate conduction transfer functions internally. This is not considered a limitation since so much programming infrastructure already exists to perform the other calculations. The temperature setpoint must also remain constant in order to develop the periodic response.

The assumption of constant temperature setpoints is a reasonable simplification in that the peak cooling load will be accurately predicted for cases where there is slight variation in the zone temperatures throughout the day in actual practice. The RTSM is not intended to predict sizing for "pick-up" loads that result from night setback conditions. While this is a limitation of the cases where the method might be applied, prior simplified cooling load calculation procedures would not be able to predict this effect either. The Heat Balance Method along with engineering judgment is required to analyze this type of scenario.

Note that typical design practice would include the allowance for start-up loads during the design of the air-handling systems, rather than the zone loads themselves.

In order to provide the most rigorous validation, the experimental facility must be designed to test these limitations for extreme cases. The test cells were specified to have a large percentage of glass surface (50% on two walls) to help detect problems with high conductance constructions. Additionally the room temperature must be able to be controlled very accurately in order to make RTSM calculations valid according to the assumed zone temperature. It would also be beneficial to study the effects of an actual periodic design day, which is closely approximated by the weather that occurs in central Oklahoma during the cooling season.

In order to design the facility, it is necessary to understand the thermal processes involved in building heat transfer. These procedures, which are discussed in the

following sections, are modeled by the Heat Balance Method and approximated by the Radiant Time Series Method.

2.3 Building Thermal Processes

All three modes of heat transfer occur in buildings: radiation, conduction and convection. Radiation and convection factor into the exterior and interior heat balances, while conduction heat transfer links the exterior and interior heat balances. Convection is the main mode of heat transfer in the air heat balance. Knowledge of all three heat transfer modes is required in order to effectively utilize either the Heat Balance Method or the Radiant Time Series Method.

2.3.1 Conduction

The general conduction problem relates heat flux through a material to its boundary conditions and material properties. In building sciences, the material properties may often be assumed constant through time and space, however the boundary conditions will change with time. For constant properties, the temperature of the outer surface will depend chiefly upon the ambient temperature of the air as well as the amount of beam and diffuse radiation falling onto the surface. Heat flux through the surface depends upon the density, specific heat, thickness, and thermal conductivity of the materials constituting the surface. Flux is proportional to conductivity and inversely proportional to thickness. Fourier's Law, shown below, quantifies conduction in terms of the temperature gradient and conductivity.

$$q'' = -k\vec{\nabla}T \qquad \textbf{(2-4)}$$

where:

q''	=	conduction heat flux	Btu/(hr·ft^2)
k	=	thermal conductivity of the material	$\frac{\text{(Btu·in)}}{\text{(hr·ft}^2\text{·°F)}}$
$\vec{\nabla}T$	=	temperature gradient	°F/ft

Fourier's Law can be applied in conjunction with the 1st law to a control volume to yield the heat diffusion equation:

$$\frac{\partial}{\partial x}\left(k\frac{\partial T}{\partial x}\right)+\frac{\partial}{\partial y}\left(k\frac{\partial T}{\partial y}\right)+\frac{\partial}{\partial z}\left(k\frac{\partial T}{\partial z}\right)+\dot{q}=\rho c_p\frac{\partial T}{\partial t} \qquad \textbf{(2-5)}$$

where:

$\dot{q}$	=	heat generation in the material	Btu/hr
ρ	=	material density	lb_m/ft^3
c_p	=	material specific heat	$\frac{\text{Btu}}{lb_m\text{·°F}}$
t	=	time, seconds	seconds
T	=	Temperature	°F
x, y, z	=	Cartesian coordinate system	ft

Equation (2-5) above, shows the heat diffusion equation in Cartesian coordinates. In building sciences, the thermal properties are often taken to be constant over the range of temperatures encountered. Incropera and DeWitt (1996) show the conductivity of several typical building materials remains constant in the temperature range experienced by buildings. This allows the simplification of Equation (2-5) to:

$$\frac{\partial^2 T}{\partial x^2} + \frac{\partial^2 T}{\partial x^2} + \frac{\partial^2 T}{\partial x^2} + \frac{\dot{q}}{k} = \frac{1}{\alpha}\frac{\partial T}{\partial t} \qquad \textbf{(2-6)}$$

where:

$\alpha = \frac{k}{\rho c_p}$ = thermal diffusivity (shown for conductivity values of BTU·in per hour·ft^2·F) $\frac{\text{in·ft}}{\text{hr}}$

The surface is not in steady state with a changing outer surface temperature. Storage of energy becomes a very important factor. Some assumptions can be made to simplify the conduction calculations. Building surfaces may be treated as a multi-layered slab. Although each layer may not be completely homogeneous (e.g. bricks and mortar or filled cell concrete blocks), any one layer or construction is typically assumed to have one set of properties. Data is available from ASHRAE and others for the most common building materials and constructions. Properties are also typically assumed for a constant and reasonable temperature – the range of temperatures encountered in building sciences is relatively small compared to the whole of physics and chemistry and for most materials their properties will not change much over that range. For most building materials no temperature dependence is even mentioned in the literature. Also for most surfaces one-dimensional heat transfer is assumed. This assumption is valid for the center of larger surfaces. The assumption is questionable where edge effects may in fact result in more extensive 2-D or 3-D heat transfer.

The Heat Balance Method assumes a multilayered slab in a transient condition with one-dimensional heat flux. If the boundary conditions are steady periodic, then periodic response factors may be applied to the problem. Non periodic boundary conditions may be solved by conduction transfer function or other numerical methods.

Storage of energy by building surfaces depends upon material properties as well. A surface with large thermal mass, defined by its density, ρ, and specific heat, c_p, will store large amounts of energy and respond slowly to changing boundary conditions. Likewise, a surface with low thermal mass will respond to changing boundary conditions quickly, and store little energy. For this reason building thermal mass is considered to be an important variable in the experiment and should be examined for at least a high and a low value. This will allow investigation of model accuracy for a wider range of conditions.

In order to reduce the experimental uncertainty associated with construction of the room surfaces, wall test sections were constructed as the facility was built. These test sections used the same materials and construction techniques as the actual building. The overall conductivity of the sections could then be measured in a guarded hot box facility. Conduction calculations for both procedures are able to utilize the measured conductivity directly, thereby reducing the uncertainty due to material property look-ups.

2.3.2 Convection

The general convection equation is:

$$q'' = h(T_s - T_{ref}) \quad \textbf{(2-7)}$$

where:

q''	=	heat flux due to convection	$Btu/(hr \cdot ft^2)$
h	=	convection coefficient	Btu/(ft2·°F)
T_s	=	temperature of the surface	°F
T_{ref}	=	fluid reference temperature	°F

Both the surface temperatures and the reference temperature can be measured in the experimental facility. For the outside heat balance, the reference temperature is the outdoor air temperature. For the inside heat balance, the reference temperature may be the bulk air temperature, the supply air temperature, or the return air temperature. The convection coefficient, however, must be measured under controlled laboratory conditions. The continuously changing boundary conditions expected in the cooling load validation test facility precludes the possibility of measuring the convection coefficient in-situ. The facility was therefore designed to accommodate the common assumptions used in generating convection correlations:

1. The test cells were located in an open area with the test cells elevated to minimize airflow disturbances. Wind velocity information from the nearby Mesonet weather station would be valid for the test cell location.
2. The interior of the test cells were constructed in the same arrangement as prior research (Fisher 1995) in order to capitalize on previously developed correlations

The construction materials selected were commonly available and configured with no fins, overhangs, etc.

2.3.3 Radiation

Since solar and thermal radiation calculations are quite complex, they are typically simplified in the cooling load calculation procedures. The degree of simplification varies depending on the process.

Emissivity, absorptivity, reflectivity and transmissivity are the basic electromagnetic properties and will vary spatially and spectrally. Typically surfaces encountered in building heat transfer can be assumed to be "diffuse" and "gray" – that is, there is no angular dependence in their properties and their emittance is assumed to be equal to their absorptivity. It is further assumed that radiation occurs through a non-participating medium. One last assumption related to electromagnetic properties is that radiation is assumed to take place in two "bands", called shortwave and longwave which correspond roughly to the visible and infrared parts of the spectrum. Solar radiation and the visible fraction of radiation from lights are considered to be shortwave, while building surfaces emit longwave radiation.

Likewise, surfaces have their properties defined for these two regions. Exterior surfaces absorb and reflect solar shortwave radiation and also participate in an infrared radiation exchange with the environment. Interior surfaces may require a shortwave absorptivity to determine the fraction of radiation absorbed from lights.

Multi-surface radiation exchange calculations can require detailed geometric input and the simultaneous solution of a large volume of non-linear equations. Simplifications are

generally made to the cooling load calculation procedure in order to make it useable in practice.

Most methods are similar in their treatment of solar radiation, utilizing empirical coefficients that determine the direct normal radiation based upon the latitude and time of year for the location of a building. Methods may vary significantly in their treatment of interior radiation exchange. Thermal radiation exchange with the environment is typically modeled according to the fundamental equations of heat transfer with a few geometrical simplifications.

Table 2-1 Spectrum of Electromagnetic Radiation

Spectrum of Electromagnetic Radiation		
Region	Wavelength (centimeters)	Energy (eV)
Radio	> 10	$< 10^{-5}$
Microwave	10 - 0.01	10^{-5} - 0.01
Infrared	**0.01 - 7 x 10^{-5}**	**0.01 - 2**
Visible	**7 x 10^{-5} - 4 x 10^{-5}**	**2 - 3**
Ultraviolet	4 x 10^{-5} – 10^{-7}	3 - 10^{3}
X-Rays	10^{-7} - 10^{-9}	10^{3} - 10^{5}
Gamma Rays	$< 10^{-9}$	$> 10^{5}$

2.3.3.1 Solar Radiation Absorbed by the Exterior Surfaces

Solar radiation is typically modeled by empirical relationships due to the atmospheric effects that could not be accurately modeled due to their transient and unpredictable nature. Solar radiation, as determined empirically, will interact with the building exterior surfaces through two modes: Direct solar radiation and diffuse solar radiation. Direct solar radiation is related to the amount of solar radiation at the surface of the earth, which can be calculated using the ASHRAE Clear Sky Model, given in Equation (2-8).

$$G_{ND} = \frac{A}{e^{\frac{B}{\sin\beta}}} \qquad \textbf{(2-8)}$$

where:

G_{ND}	=	direct normal solar radiation	Btu/(hr·ft^2)
A	=	apparent solar irradiation	Btu/(hr·ft^2)
B	=	atmospheric extinction coefficient	Btu/(hr·ft^2)
β	=	solar altitude angle	degrees or radians

Typical monthly values for A, B and β are shown in ASHRAE (2005) and McQuiston and Spitler (2000). The 21st day of the month can be assumed to be a representative day for load calculations.

The value of the direct radiation calculated using Equation (2-8) must be adjusted to find the portion of the radiation that is normal to the surface using solar angle calculations. Diffuse radiation is calculated according to Equation (2-9), utilizing the clearness of the

sky. Atmospheric clearness numbers for summer and winter are also available from ASHRAE (ASHRAE 1989) for a wide range of locations in the United States.

Some portion of the solar radiation incident on a surface will be diffuse radiation, which is inversely related to the clearness, i.e. on a cloudy day a higher percentage of the solar radiation will be diffuse. A formulation for diffuse radiation is shown below in Equation (2-9). The coefficient, C, is also found in ASHRAE (2005).

$$G_d = C\frac{G_{ND}}{C_N^2} \quad \textbf{(2-9)}$$

Equation (2-9) can be combined with the normal radiation of a surface in Equation (2-10) to form one equation for direct radiation on a surface, shown in Equation (2-11).

$$G_D = C_N G_{ND}\cos\theta \quad \textbf{(2-10)}$$

$$G_t = G_D + G_d = \left(\cos\theta + \frac{C}{C_N{}^3}\right) C_N * G_{ND} \quad \textbf{(2-11)}$$

Where:

G_D	=	Direct solar radiation	Btu
C_N	=	Clearness number, normal	–
G_{ND}	=	Normal, direct solar radiation	Btu
θ	=	Angle of incidence	Degrees or radians
C	=	Clearness number	–

The test cell's location near a Mesonet weather station will allow the usage of measured solar radiation quantities. The Heat Balance Method is capable of using either measured solar radiation quantities or calculating solar radiation based upon the observed cloudiness conditions. The RTSM uses a sol-air temperature to account for the combined effect of solar radiation and the outdoor air temperature. The sol-air temperature is covered in more detail in following sections.

2.3.3.2 Longwave Radiation Exchange with the Environment

Radiation exchange with the environment depends upon the temperature of the building surface and temperature of the environment. In the simplest case this is an elementary radiation heat transfer problem. In actuality, the environment may consist of numerous surfaces all at differing temperatures and with different view factors to the building surface.

Error! Objects cannot be created from editing field codes. **(2-12)**

Where:

$q''_{radiation,out}$	=	Net radiation exchange of the surface with the sky and ground	W/m^2
ε	=	Emissivity	-
σ	=	Stefan-Boltzmann Constant	$\frac{W}{m^4 \cdot K^2}$
F_{s-g}	=	View factor from the surface to the ground	-
F_{s-sky}	=	View factor from the surface to the sky	-
T_s	=	Temperature of the surface	K
T_g	=	Temperature of the ground	K

The view factors can be calculated based upon the known geometry. The equation uses absolute temperatures, which are required for radiation exchange calculations.

In cooling load calculations, Equation (2-12) will typically be linearized in order to simplify the computational procedure. In order to validate the procedure, both environmental temperatures and view factors must be estimated. The experimental facility was elevated and constructed in the middle of an empty field such that few assumptions about radiation exchange would be required.

2.3.3.3 Fenestration

The Solar Heat Gain Coefficient (SHGC) model is provided in the ASHRAE Handbook of Fundamentals. The SHGC depends upon the geometry and optical properties of the window and can be quite difficult to estimate by hand. Lawrence Berkeley National Laboratory (LBNL) developed the WINDOW program with the aid of several window manufacturers. The WINDOW program will output the optical parameters necessary to calculate the fenestration heat gain for both the Heat Balance Method and the RTSM.

The sunlit area of the window is first calculated using the solar angle calculations and the geometry of the window and its reveals, overhangs and fins. The beam solar radiation is calculated from the incident angle and the sunlit area and the diffuse radiation is calculated from the ground and sky parameters. The transmitted energy is then the beam radiation multiplied by the solar transmittance for that hour and the diffuse radiation multiplied by the hemispherical transmittance. The portion of the solar energy that is absorbed by the glass and subsequently seen as a gain by the space is calculated as the

solar radiation that enters the glass by absorption and modified by the inward flowing fraction as specified as a parameter. Absorption by both beam and diffuse radiation are calculated.

The test cells were constructed with the simplest windows available to minimize any discrepancies between modeled and actual values due to assumptions and manufacturing variation. The geometry of the test cells was such that there would be no shading from external objects. The windows were configured so that interior shading devices could be tested in future experiments. Initially, the tests were performed with no interior shades.

2.3.3.4 Interior Radiation

The Mean Radiant Temperature (MRT) model formulated by Walton (Walton 1980) makes a simplification that all of the surfaces of a thermal zone are participating in radiation exchange with one equivalent surface. The electromagnetic and physical properties of the equivalent surface can be calculated according to Equations (2-13), (2-14) and (2-15). All equations regarding the MRT model utilize Rankine temperatures as presented, but could easily be converted to SI units.

$$A_{MRT_i} = \sum_{i \neq j}^{n} A_j \tag{2-13}$$

$$\varepsilon_{MRT_i} = A_{MRT_j} \sum_{i \neq j}^{n} A_j \varepsilon_j \tag{2-14}$$

$$T_{MRT_i} = A_{MRT_j} \sum_{i \neq j}^{n} \frac{\left(A_j \varepsilon_j T_j\right)}{\varepsilon_{MRT}} \tag{2-15}$$

Where:

A_i	=	Area of each surface	ft^2
T_i	=	temperature of each surface	°R
ε	=	Emissivity of each surface	–

Radiation will be exchanged amongst all of the surfaces and the equivalent surface (also known as the "fictitious" surface according to Equations (2-16) and (2-17) below:

$$q''_{MRT_i} = \sigma F_{MRT_i} \left(T_i^4 - T_{MRT}^4\right) \tag{2-16}$$

$$A_i F_{MRT_i} = \frac{1}{\frac{1-\varepsilon}{A_i \varepsilon_i} + \frac{1}{A_i F_{i,MRT}} + \frac{1-\varepsilon_{MRT_i}}{A_{MRT_i} \varepsilon_{MRT_i}}} \tag{2-17}$$

and if $F_{i,MRTi} = 1$, then Equation (2-17) above can be simplified to Equation (2-18).

$$F_{MRT_i} = \frac{1}{\frac{1}{\varepsilon_i} + \frac{A_i\left(1-\varepsilon_{MRT_i}\right)}{A_{MRT_i} \varepsilon_{MRT_i}}} \tag{2-18}$$

It is common to modify the MRT method with a correction term in order to force the sum of the radiation exchange terms to sum to zero. It is also typical to linearize the non-linear terms in the equation by factoring out (T_i-T_{MRTi}) as in Equation (2-19) below:

$$T_i^4 - T_{MRT_i}^4 = 4T_{MRT_i}^3 \left(T_i - T_{MRT_i}\right) \tag{2-19}$$

The Heat Balance Method can utilize any number of radiation exchange algorithms, however the MRT Balance method is particularly appealing based on a balance of the level of accuracy desired with the data inputs that are well known and the computational intensity of the method. The RTSM attempts to capture the effect of the radiant exchange in the radiant time factors, which are generated by a heat balance procedure.

2.3.4 Internal Gains and Infiltration

People and equipment heat gains are important contributions to the cooling load. People reject sensible and latent energy to the space depending on their activity level and other factors. Equipment generates heat through normal mechanical and/or electrical operation.

Sensible heat from people and equipment can be introduced to the space through two modes, convection and radiation. Convective gains are seen immediately as a cooling load in the space. Energy transferred to the surfaces in the space by radiation will become a cooling load at a later time when it is convected from the surfaces. The stored energy will be radiated to the other surfaces according to Equation (2-2). It is very difficult to generalize the ratio of convected to radiated energy for these gains, particularly for people gains that are not necessarily constant throughout time. ASHRAE (ASHRAE 2005) provides some guidelines for determining the radiative/convective split.

Internal gains from equipment are very easy to model in a cooling load procedure. The convective portion is simply added to the heat extraction performed by the air system. The radiative portion participates in the surface heat balance in the Heat Balance Method and is operated on by radiant time factors in the RTSM.

In order to accurately validate the cooling load calculation procedures, the internal gains—especially the convective gains—should be minimized. The cooling load can easily be dominated by convective gains from internal loads. Since these gains are simply added to the cooling load, they have the effect of masking the true effectiveness of a cooling load procedure. Figure 2-3 below contrasts two scenarios with high and low internal convective gains by percentage of total cooling load.

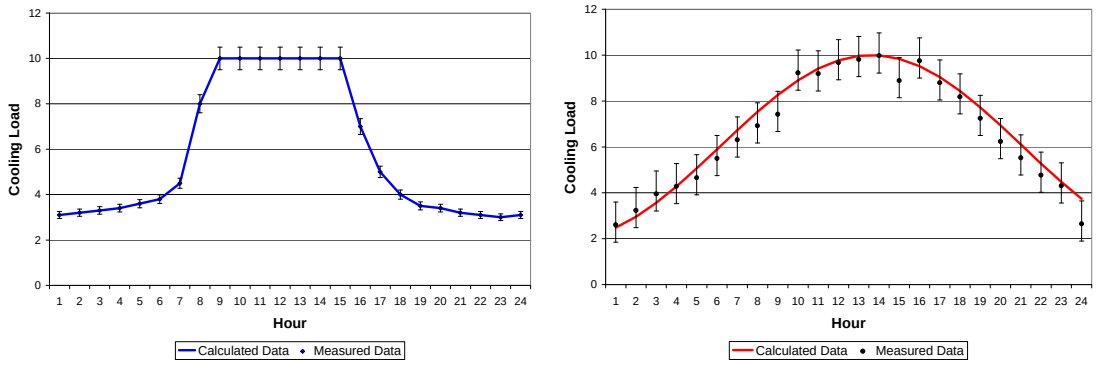

Figure 2-3 Two convective internal gains cases

The figure on the left depicts a zone with high internal convective gains during mid-day hours. The calculated and measured data points drop right on top of each other due to the dominance of the known internal convective gains. The figure on the right shows a

building where the dominant gains are envelope related which will allow some forensic analysis of component cooling load models.

In a similar fashion, infiltration could affect the validation in the opposite way as the models require inputs that may not be known before construction and will be difficult to accurately determine for projects still in the design phase.

For the test facility, infiltration was measured in order that the gains due to infiltration could be input directly to the cooling load rather than use any of the infiltration models available in the literature.

Both the RTSM and Heat Balance Method assumed zero internal gains from equipment, lights and people for this validation project. Infiltration was assumed to be 0.19 air-changes per hour for both buildings in accordance with experiments performed for this purpose. No analytical infiltration models were used during the validation experiments.

Chapter 3

Design and Construction of Experimental Facility

3.1 Design Criteria

In order to validate the methods the facility was designed to minimize instantaneous convective heat gains and increase the relative magnitude of radiation and conduction heat gains. In addition, it was necessary to design a facility that could be accurately described in terms of model input parameters. The three overriding design criteria were therefore a measurable thermal mass effect, measurable solar effect and well-defined model parameters.

3.1.1 Measurable Thermal Mass Effect

Thermal mass is an important parameter in building heat transfer. A building that has relatively little or no thermal mass will tend to behave almost in steady state heat transfer. As thermal mass is added, transient effects become more pronounced. Increased thermal mass will provide energy storage, which will have two main effects in a cooling load calculation. First, as energy is absorbed by the thermal mass the instantaneous cooling load will become smaller in magnitude. Second, as that energy is gradually released into the space a lag will develop between the peak heat gains and the peak cooling load. The test facility was designed so that the effects due to thermal mass would be emphasized. Two test cells, one of brick and filled core concrete block, and one of studs and insulation allowed a direct comparison between measured and predicted cooling load for high and

low mass buildings with the same environmental conditions. Due to the high percentage of glazing in each test cell, the quantity of instantaneous heat gain is high resulting in small differences between the peak hours for the two buildings, as shown below in Figure 3-1. However, the theoretical plots below show a significant time lag between peak hours in the cases without windows, demonstrating the effect thermal mass can have if the cooling load is not dominated by other instantaneous heat gains.

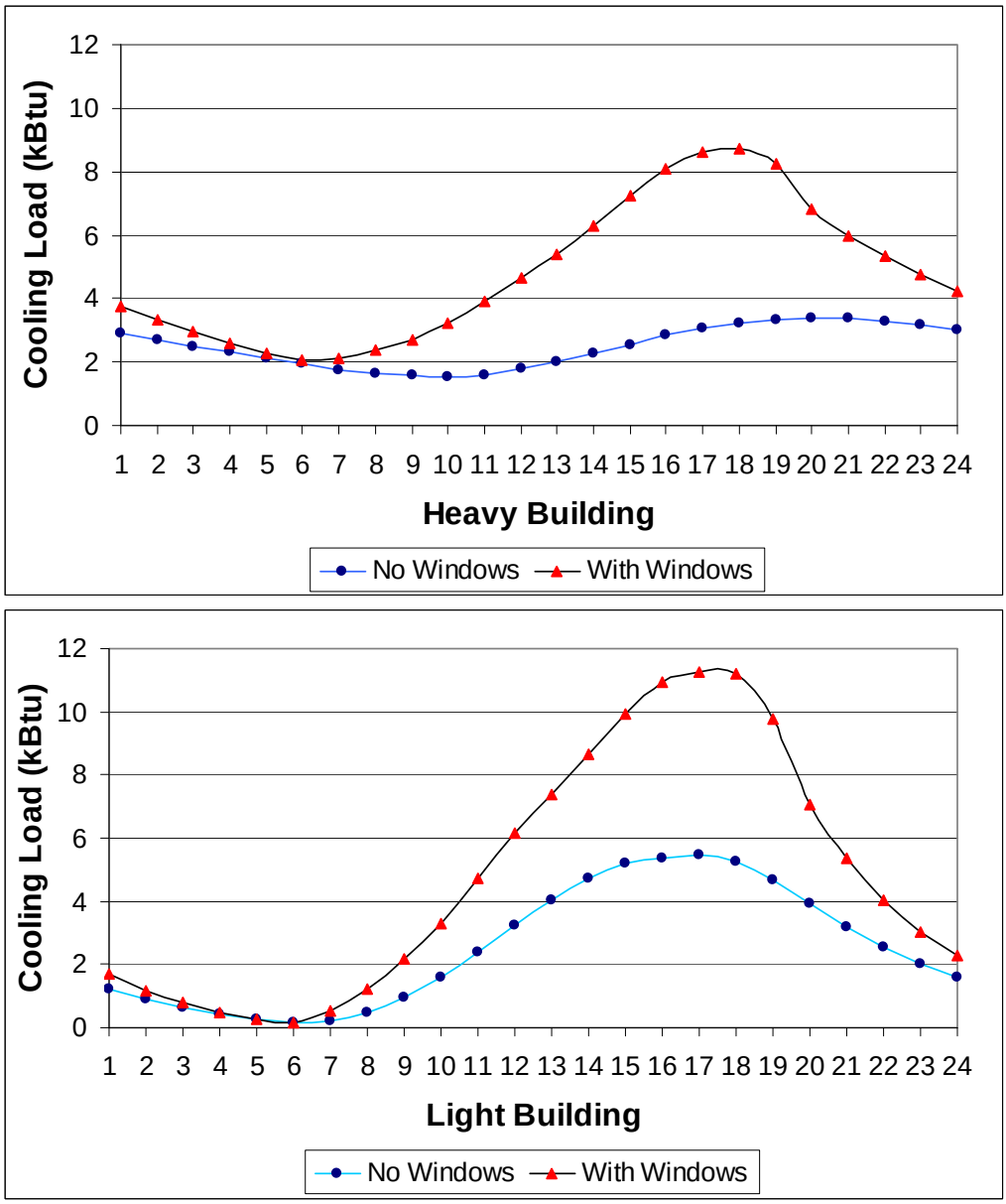

Figure 3-1 Modeled cooling loads for each test cell, glazed and un-glazed

3.1.2 Measurable Solar Effect

Another important part of any cooling load calculation procedure is how radiant gains are handled. Measurable solar effect was produced by constructing the test cells with large (50% of gross outside wall area) windows on the South and West faces of the buildings.

The buildings were also constructed with a passive floor. Picture 3-1 shows a photograph of the elevation for test cells. (Photo is of heavy thermal mass building only.) Decoupling the test cells from the ground allowed an assumption that the floor would not participate in heat transfer with the ground. Transmitted solar radiation incident on the floor would be kept within the space. The floor does still store energy which will eventually be radiated to the space. The experimental setup ensured that negligible heat transfer would occur to the control room by insulating the floor slab on the ceiling of the control room. In this way the control room will act like a "guard" space.

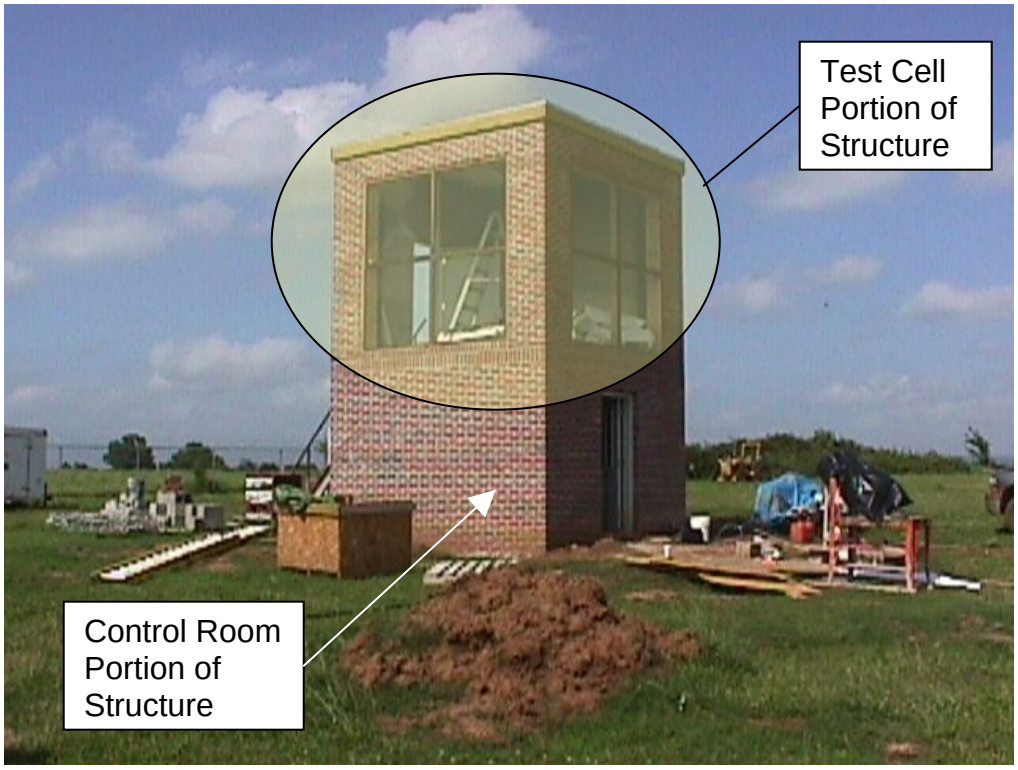

Picture 3-1 Heavy Building with Test Cell Portion Indicated

3.1.3 Estimation of Model Input Parameters

There are two sources of error in a load calculation. The first source of error is incorrect inputs to the models. "Garbage In, Garbage Out" (GIGO) is a mantra of computer programmers everywhere. Error can also be due to over-simplified or incorrect models. The objective of the test facility was to eliminate the first source of error to the greatest extent possible and measure the second source of error.

3.1.3.1 Estimation of Physical Properties

Solar Absorptivity

Solar absorptivity is determined by measuring the temperature of a surface and the emitted radiation from that surface. A net radiometer was used to estimate the solar absorptivity of the surfaces of the test cell.

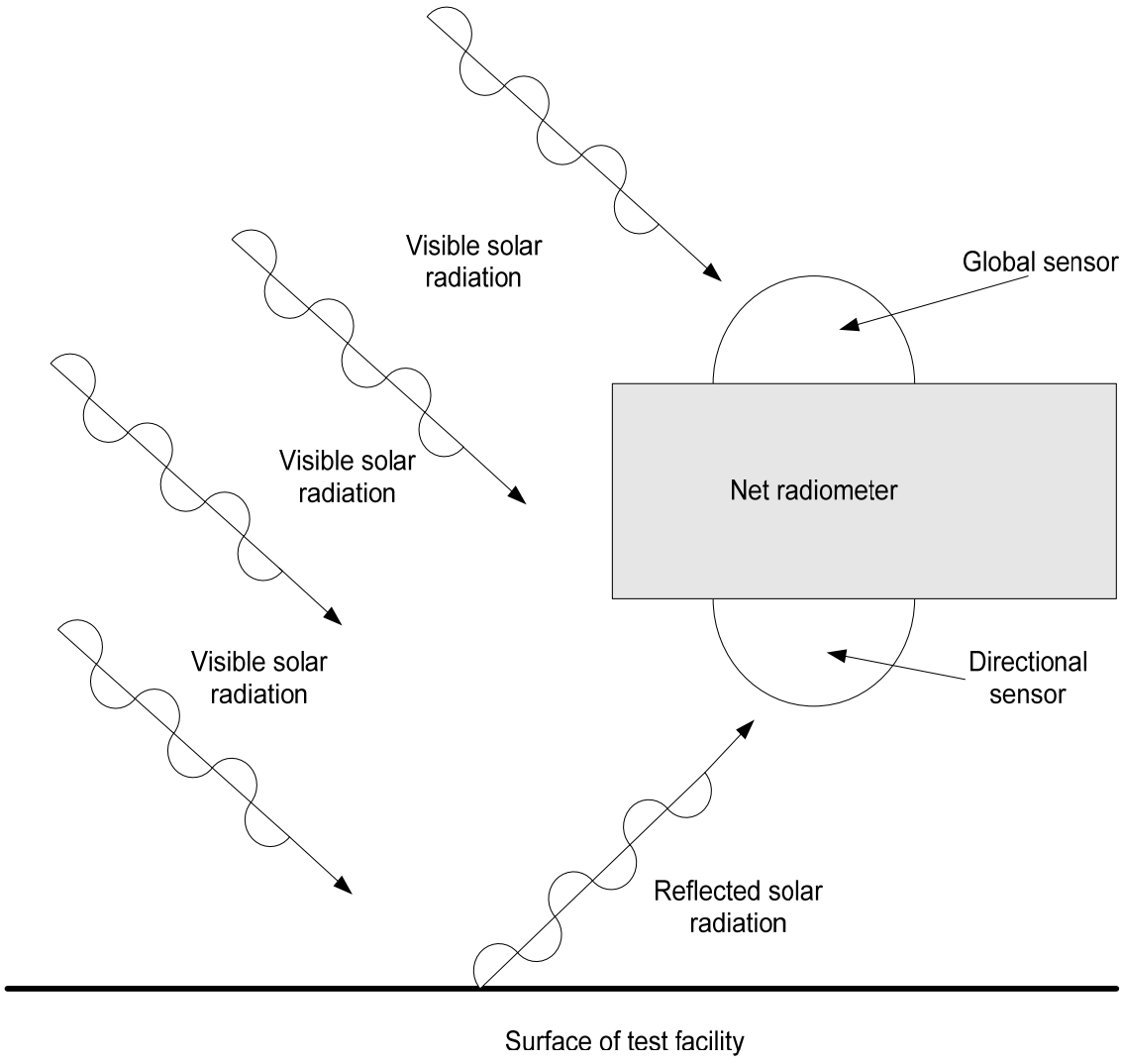

Figure 3-2 Net radiometer

Picture 3-2 Net radiometer and pyronometer with shadowband

Thermal Conductivity

Conduction in building heat transfer is typically assumed to be one-dimensional. The reality is that there will be some 2-D heat transfer, particularly around edges and corners. The vast majority of heat transfer will be included in the assumption of one-dimensional flow for a typical building surface. Assuming 1-D flow, the temperature at the surface of a material can be estimated from response factors. Response factors cannot be measured as they are not a physical property of the material. In the special case of a steady state surface, the twenty four response factors will sum to be the U-value of a construction, providing a "sanity check" between the sum of the response factors and the total daily conduction heat transfer under a steady periodic condition.

Thermal conductivity of the test cell walls was determined through a steady state test by subjecting the wall constructions to a known heat flux and calculating the overall heat transfer coefficient for the wall section. This process was commissioned as a Senior Capstone Design project under the Mechanical and Aerospace Engineering Department. The results of this project factored directly in the RTSM validation paper written by Iu et al. (2003) and the Heat Balance Method paper written by Chantrasrisalai et al. (2003).

A facility to measure transient conduction and estimate thermal response factors was not available. The uncertainty associated with the parameters was somewhat minimized by using materials with well-defined densities and specific heats.

3.1.3.2 Direct Measurement of Environmental Parameters

Weather data are a significant portion of input for many building simulations. Weather data files are available for analysts to choose from when working on simulation projects. The validation project however required that weather data be accurately estimated. Measured weather data including incident solar radiation, air temperature and wind vectors were available from a nearby Mesonet station and on-site pyronometers.

Solar Radiation

Solar radiation is on the whole accurately predicted by component models available in the literature. Models exist that have been shown to accurately calculate the incident beam radiation on a surface based upon the date and time for a given geometry. Load calculations can use these models to calculate insolation for any surface. The models are not able to account for local anomalies due to inconsistent weather. The Heat Balance Method calculates the solar radiation entering the atmosphere for a clear day. A clearness factor can be used to simulate cloudiness; however, this is only an approximation to complex weather phenomena. A design day calculation on the other hand uses the maximum solar radiation possible for any given hour and is not concerned about anomalies that might slightly reduce the calculated load. An accurate validation facility should have the capacity to measure the solar radiation as it occurs at the experimental site. The test cells are equipped with solar instrumentation, and additionally a state of Oklahoma supported weather network station is located nearby with data that is available to researchers and students. The weather station records data every five minutes with the data made available by ftp server on a daily basis.

Infiltration

Infiltration models must be experimentally developed for specific buildings. Programs and models are available, however many of the parameters are difficult to estimate. The ASRHAE Crack Method (McQuiston and Spitler 2000) is shown below in Equation (3-1):

$$\dot{Q} = A \times C \times \Delta P^{n} \quad \textbf{(3-1)}$$

All four parameters must be determined experimentally and may vary over a wide range depending on construction characteristics of the building, prevailing wind velocity, air temperature gradients and pressure gradients induced in the building by the environment and/or the installed mechanical systems. The infiltration rate can be measured at a particular point in time, however for simulation purposes it would clearly be beneficial to construct the facility in such a way as to minimize the rate of infiltration, perhaps even make it negligible. In the case of the test cell, the building was designed to be "air-tight." Testing and resealing was performed to minimize infiltration then CO_2 tests were performed to model infiltration rates as a function of wind speed, as shown in Section 6.2.

Outdoor Air Temperatures

Outdoor air temperature is a critical parameter in the determination of conduction heat gain through a building surface. The outdoor dry-bulb temperature is a direct input to the heat balance model. The outdoor temperature is logged at the nearby Mesonet weather station.

3.2 Building Envelope

3.2.1 Site Plan

The location of the buildings is Stillwater, OK. The latitude is 36° 8'9.16"N and the longitude is 97° 4'51.07"W. The building orientation was corrected from magnetic to true north (~3.5 degree correction). The standard meridian for the USA central time zone is 90°. The two test cells are oriented one directly north of the other. The test cells are oriented so the surfaces all face directly in a major compass point direction. The distance between the buildings is 35 feet. The minimum distance for no solar interaction was calculated to be 25 feet using the ASHRAE Loads Toolkit (Pedersen 2001) solar angle subroutines. The distance of 35 feet is more than enough to ensure that the south building will not cast shade upon the north building. A solar measurement stand is located approximately 25 feet southwest of the south building. The stand is not tall enough to cast a shadow on the test cells. A diagram of the site arrangement is shown in Figure 3-3.

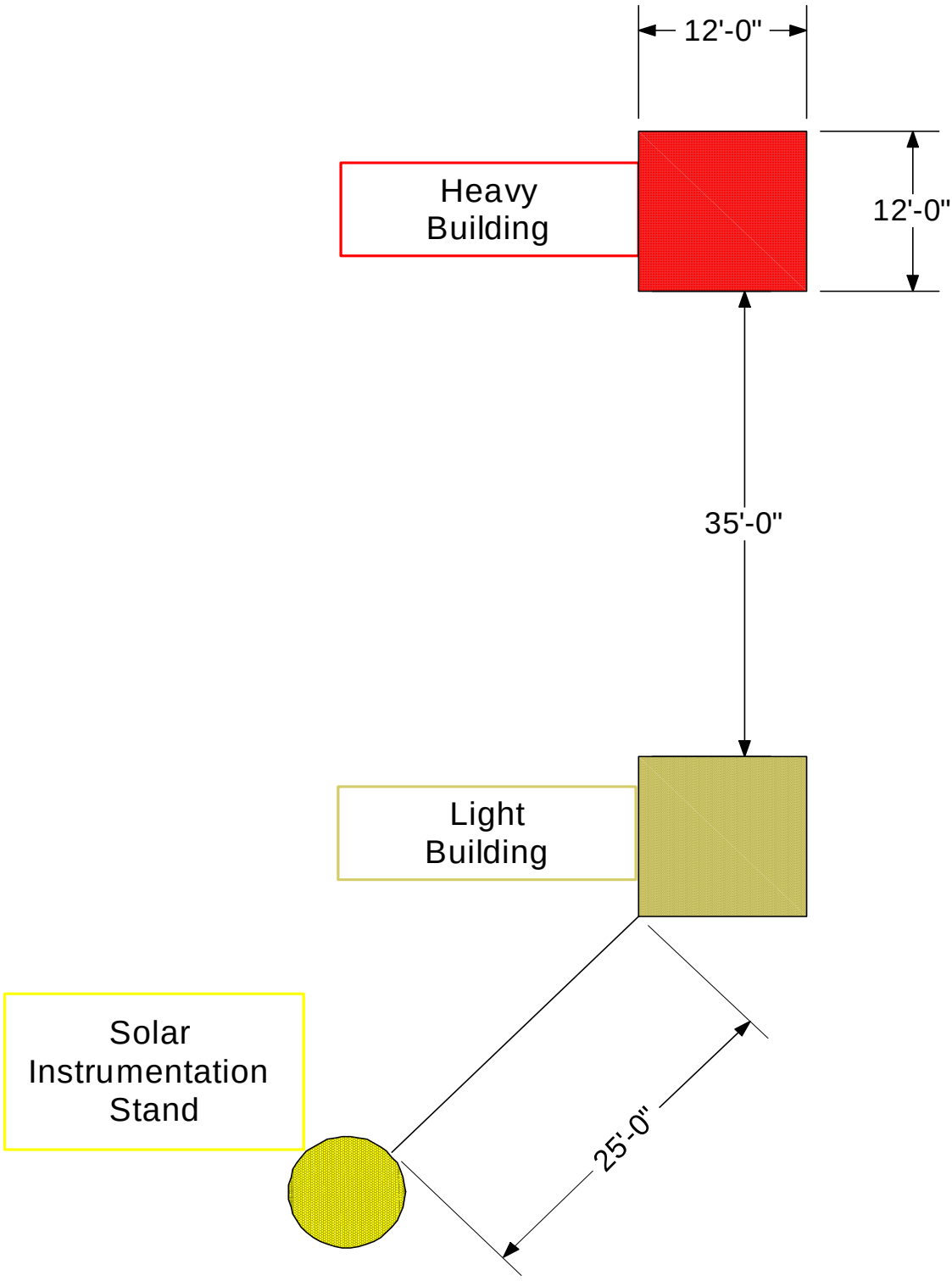

Figure 3-3 Experimental facility site plan

The buildings were constructed in a two-story fashion such that the test cell portion of each building is on the second story. By decoupling the test cell from the ground, the uncertainty associated with the ground heat transfer calculations was eliminated. Also transmitted solar radiation incident on the floor that was absorbed would not be conducted through to the ground or the chamber below. The first floor level of each building was used as the control room. This space is conditioned both to keep the computer equipment in working order as well as to act as a "guard space". Additionally, insulation was added to the ceiling of the control room to minimize heat transfer between the rooms. A schematic of the facility is shown in Figure 3-4. Air is supplied to the test cell through a penetration in the floor slab of each building. The supply air temperature is measured in an insulated duct protruding into the test cell. The control volume is shown in Figure 3-5. The return air temperature is measured at the slab level. Both buildings have their own forced air system and data acquisition system. The air systems are identical, consisting of a ground source heat pump, air measurement section, ground loop reheat, electric reheat, a phase angle fired SCR, and a temperature controller. The supply and return air temperatures are measured by thermocouple grids installed in the ducts. This and other instrumentation will be discussed in Chapter 4.

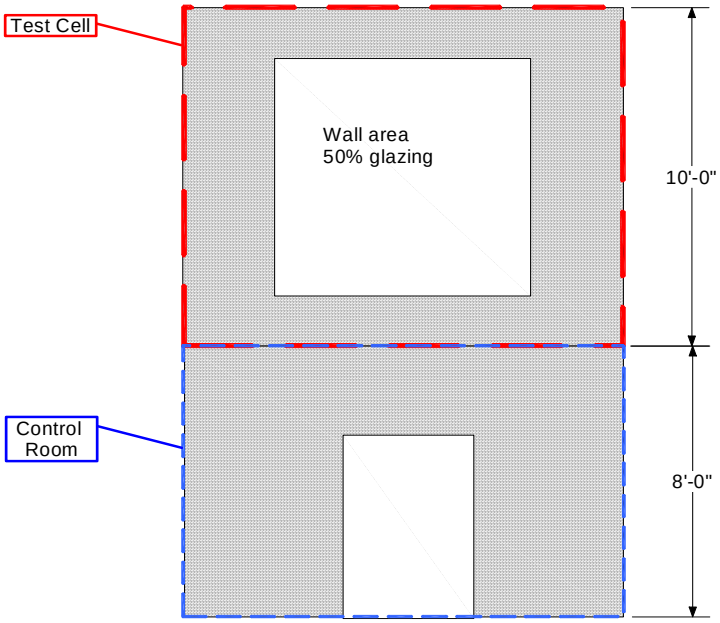

Figure 3-4 Test cell and control room arrangement

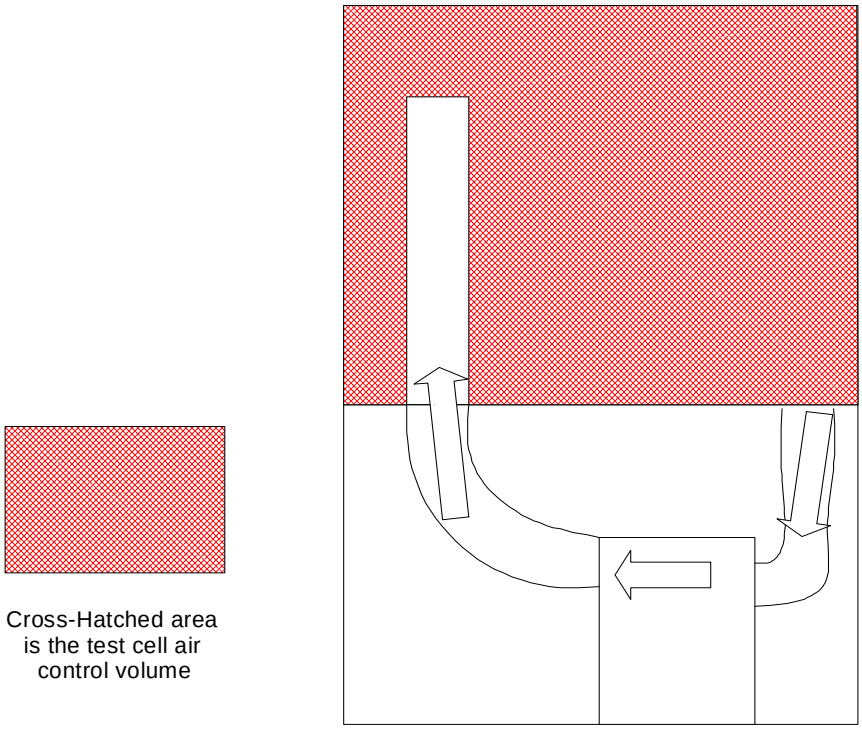

Figure 3-5 Test cell air control volume with air flow direction

3.2.2 Test Cell Structural Design

A steel superstructure, as shown in Figure 3-6, supports the buildings. The top and bottom decks and the ground slab extend beyond the columns to minimize conduction heat transfer from the outside through the building steel. A concrete roof was poured on the heavy building as discussed in the following section. The roof of the lightweight building was a built-up insulated roof. Both test cells have poured concrete floors, each of a different thickness.

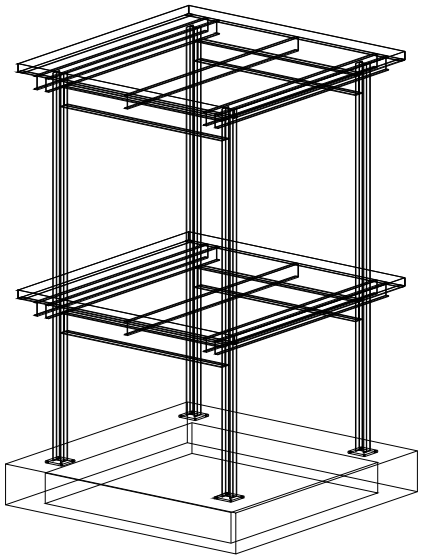

Figure 3-6 Building steel superstructure

Figure 3-7 shows a plan view of the structural design. A nominal 12' was used for exterior wall sizing based on inside and outside dimensions.

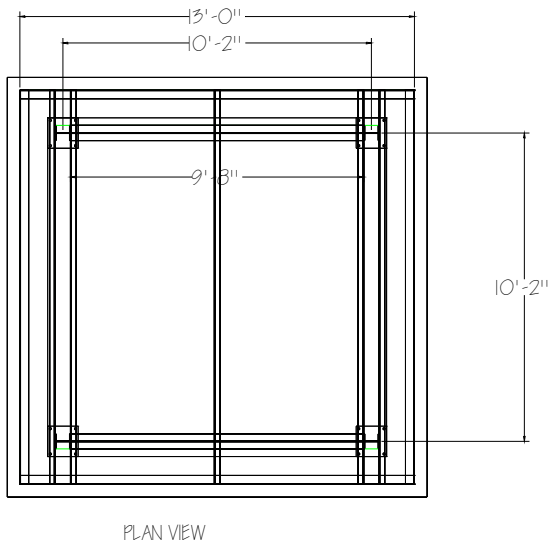

Figure 3-7 Plan view of structure

3.2.3 Heavy Building

Construction

The walls of the heavy building are made of four inch face brick, two layers of half inch extruded polystyrene foam board insulation, and filled eight inch heavyweight concrete blocks as shown in Figure 3-8. A moveable wall section was built in the laboratory by the same mason that constructed the test cell walls. This portable (although quite heavy!) wall section is suitable for laboratory measurement of overall wall thermal properties.

The roof of the heavy building, shown in Figure 3-8, is made of a shingle roll placed on top of tarpaper. Next there is a layer of 7/16-inch Oriented Strand Board (OSB) and two inch layers of extruded polystyrene foam board. There is another 7/16-inch OSB layer, and then four inches of concrete. The concrete is on top of a piece of metal decking,

approximately 1/16 inches thick. The floor of the heavy building is five inches of concrete poured on top of the metal decking.

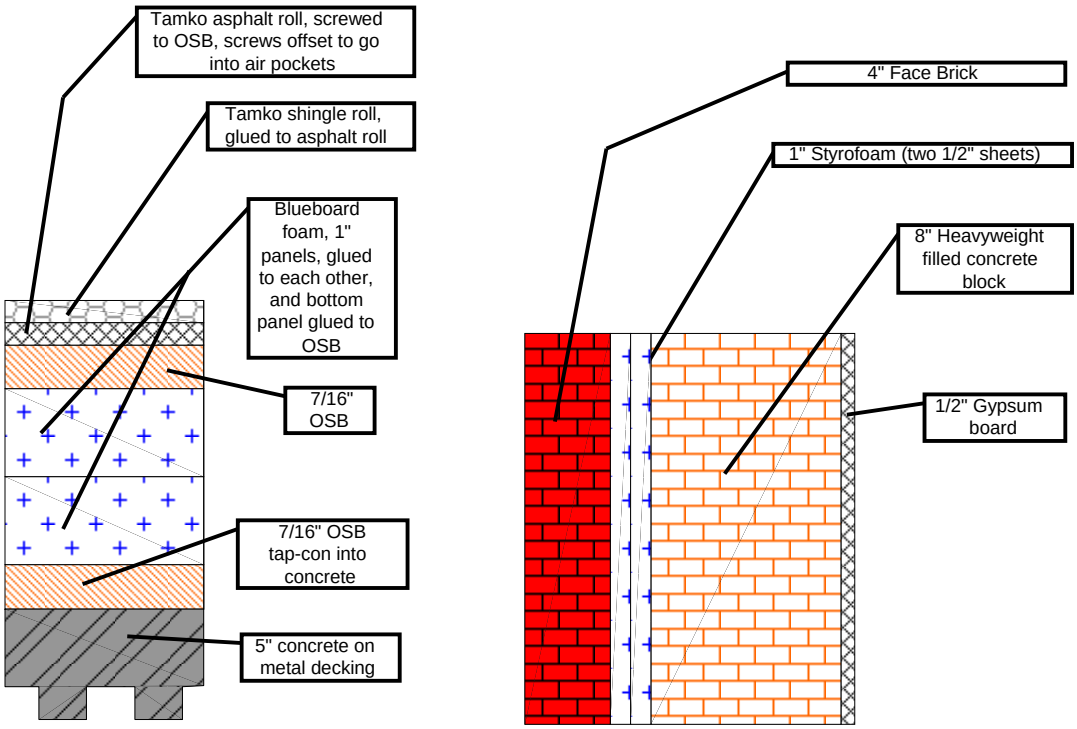

Figure 3-8 Heavy building roof (left) and wall (right) construction

Thermal Properties

The thermal properties of the building materials are critical inputs to the cooling load calculation procedures. Both the Heat Balance Method and the RTSM use the material properties to calculate the conduction transfer functions and periodic response factors used in the conduction calculation. Table 3-1 shows the material properties for the heavy building.

Details of Building Materials for North (Heavyweight) Building					
Type of Construction	Description of Layers (from Outside to Inside Surfaces)	Thickness	Thermal Conductivity	Density	Specific Heat
		ft	Btu-in/h-ft2-F	lbm/ft3	Btu/lbm-F
Walls	4" Face Brick	0.33	11.67	125.13	0.22
	1" Extruded Polystyrene	0.08	0.25	2.00	0.29
	8" HW Concrete Block filled w/ HW Concrete	0.67	15.16	140.19	0.20
	1/2" Gypsum Board	0.04	6.37	100.13	0.20
Roof	Shingle Roll	0.00	0.32	68.75	0.36
	Tar Paper	0.00	0.11	68.75	0.30
	7/16" OSB/Plywood	0.04	1.02	33.75	0.29
	2" Extruded Polystyrene	0.08	0.25	2.00	0.29
	7/16" OSB/Plywood	0.04	1.02	33.75	0.29
	5" Concrete	0.42	1.51	40.06	0.20
	Metal Decking	0.01	394.05	480.56	0.10
Floor	Metal Decking	0.01	394.05	480.56	0.10
	5" Concrete	0.42	1.51	40.06	0.20

Table 3-1 Heavy Building Material Properties

3.2.4 Light Building

Construction

The walls of the light building are constructed according to Exterior Insulation Finish System (EIFS) specifications. The outermost layer is a type of stucco. Beneath that is a layer of 1 inch expanded polystyrene Styrofoam™ beadboard. This is next to a layer of 7/16-inch OSB. The next layer is a parallel combination of 2" x 4" studs and 4 inch

fiberglass batt insulation. The innermost layer is a half-inch sheet of gypboard. A schematic of the light building wall is shown below in Figure 3-9.

The roof of the light building, below in Figure 3-9, is made of a shingle roll placed on top of tar paper. Next there is a layer of 7/16-inch Oriented Strand Board (OSB) and two one-inch layers of extruded polystyrene foamboard. There is another 7/16-inch OSB layer, and then metal decking. The floor of the light building is 3.5 inches of concrete poured on top of the metal decking.

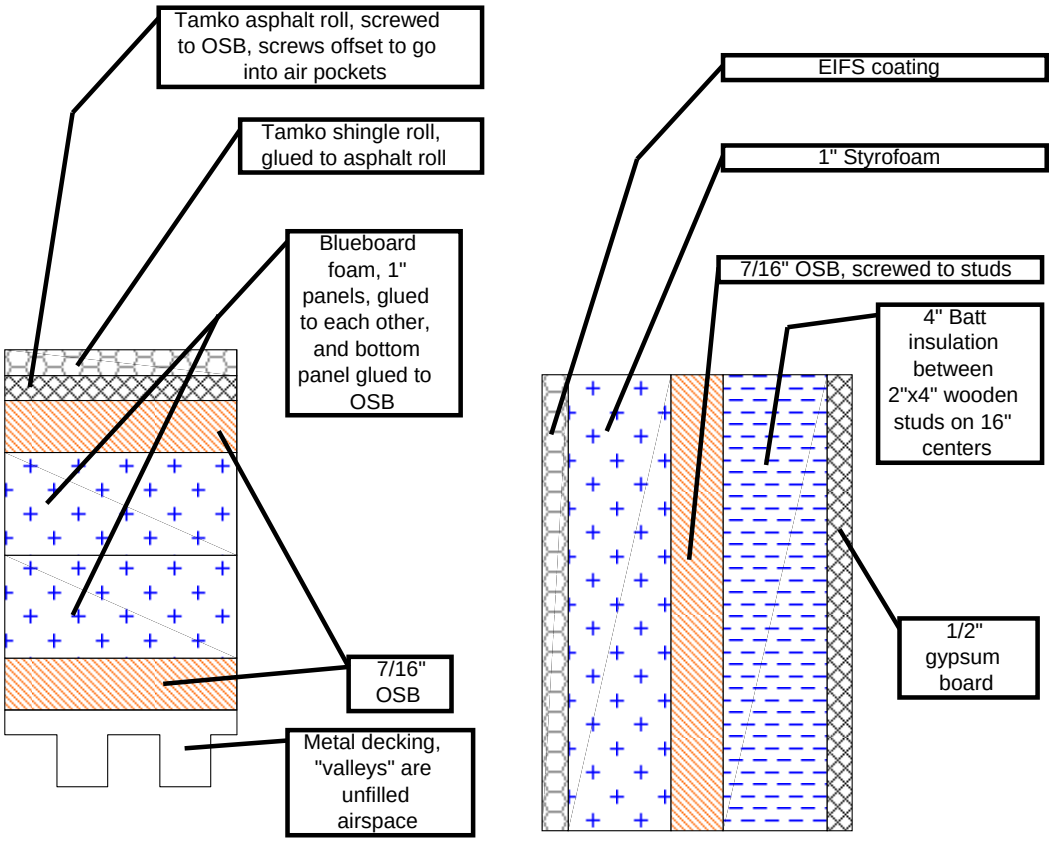

Figure 3-9 Light building roof (left) and wall (right) construction

Thermal Properties

The thermal properties of the lightweight building are shown in Table 3-2. Although the materials used in the two buildings were quite different, the overall U-values of corresponding heat transfer surfaces were similar.

Details of Building Materials for South (Lightweight) Building					
Type of Construction	Description of Layers (From Outside to Inside Surfaces)	Thickness	Thermal Conductivity	Density	Specific Heat
		ft	Btu-in/h-ft2-F	lbm/ft3	Btu/lbm-F
Walls	1/4" Stucco	0.02	6.06	116.13	0.20
	1" Styrofoam (Expanded Polystyrene)	0.08	0.25	2.00	0.29
	7/16" OSB/Plywood	0.04	1.02	33.75	0.29
	3 1/2" Fiberglass Insulation	0.29	0.32	6.00	0.23
	1/2" Gypsum Board	0.04	6.37	100.13	0.20
Roof	Shingle Roll	0.00	0.32	68.75	0.36
	Tar Paper	0.00	0.11	68.75	0.30
	7/16" OSB/Plywood	0.04	1.02	33.75	0.29
	2" Extruded Polystyrene	0.08	0.25	2.00	0.29
	7/16" OSB/Plywood	0.04	1.02	33.75	0.29
	Ceiling Air Space	0.00	0.00	0.00	0.00
	Metal Decking	0.01	394.05	480.56	0.10
Floor	Metal Decking	0.01	394.05	480.56	0.10
	3.5" Concrete	0.29	1.51	40.06	0.20

Table 3-2 Light Building Material Properties

3.2.5 Windows

The windows cover 50% of the outside area of their respective walls as shown in Figure 3-4 and are constructed from 3/16 inch single pane clear glass. At the time that the EIFS was applied to the light building eight panels with the same dimensions as the windows were covered with the coating. These panels could then be used to replace the windows for a test that required a smaller amount of glazed surface. The panels are also suitable for testing to determine the overall heat transfer coefficient of the EIFS wall construction. The framing area of the brick building windows was constructed out of

wood with a structural steel lentil across the top, allowing for the brick windows to be filled in during future testing.

The windows were designed to represent 50% of the wall surface in order to maximize the solar heat gain. Four panes of glass were individually screwed into the center of the south and west walls in each test cell. A typical detail for windows in included below in Figure 3-10.

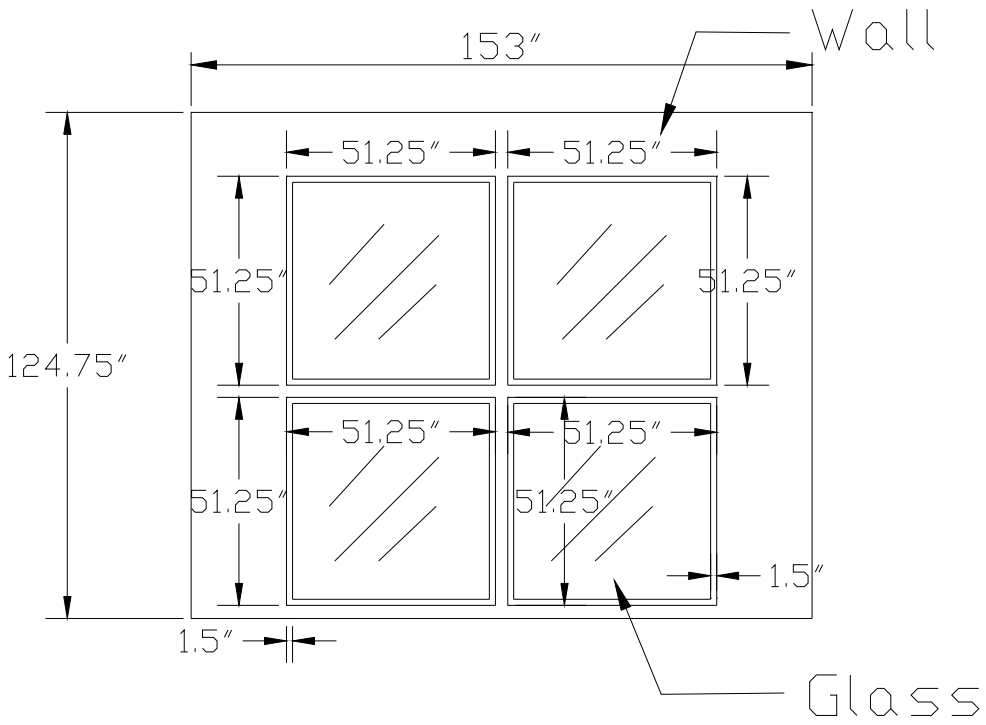

Figure 3-10 Typical window detail

The window frames were screwed into wooden parts such that there were no thermal breaks. Several layers of sealant were applied to the frames in order to minimize

infiltration though the cracks around the window construction. The total glazing for any one wall consisted of four panes of glass. Each pane was an inoperable individual pane and frame in order to minimize infiltration through mechanical constructions.

Single pane glazing was chosen to provide the most basic input to the models. This type of glazing is not typical for most construction today. Typical glazing would result in a lower heat gain from fenestration. This project required large heat gains from the building components to enhance the procedure validation.

3.3 Building Air System

3.3.1 Air Distribution System

The supply air routing was identical for both test cells. The supply air was provided from a single radial diffuser located in the center of the test cell, ten feet above the floor. Tests would be performed both with and without a drop-ceiling installed. The duct rose through the floor, up to the roof and then to the center of the room using two elbow sections. The return penetration was located in the northeast corner of the floor slab. The return air duct runs straight down to the heat pump below. A second fan was placed in series in the return air ductwork after initial experiments showed the need for higher airflow.

3.3.2 Ground Source Heat Pumps

The system consists of a Florida Heat Pump GT 018 model geothermal heat pump. Its nominal cooling capacity at standard air and water temperature is 18,000 Btu/h. This unit was selected for its nominal capacity that is slightly higher than the peak load the

buildings were predicted to experience. The heat pump is connected to two vertical bore U-tubes, 250 feet deep using 1 inch HDPE pipe

3.3.3 System Operation and Controls

3.3.3.1 Heat Pump Operation

The heat pump compressor runs 100% of the time. This is necessary to provide the temperature stability required to control the room air temperature to within ± 0.5 °C. The heat pump reversing valve is never switched to heating mode, if there is a net heating load that energy is provided by one or both of the reheat coils.

3.3.3.2 Electric Reheat

An electric heating coil provides reheat to the air stream. Since the heat pump compressor runs all of the time, some degree of reheat is also needed all of the time. The benefits of electric reheat are that it is flexible in its implementation and has a quick response. The capacity of an electric coil is variable depending on voltage and coil resistance and therefore can be accurately chosen. Alternatively, an electric reheat coil can be difficult to control. There are two methods of controlling an electric heating coil. The most common method is to pulse the coil with voltage using either a relay or silicone controlled rectifier (SCR) in zero cross-firing mode. This method works on the principle of a duty cycle, where the desired power is approximated by powering the coil at full line voltage for a percentage of a given time period. The second method is to use a phase angle firing SCR. This type of SCR chops the waveform to provide a level voltage that is less than or equal to the line voltage. This type of controller requires a transformer on the

same phase as the controller. Care must be taken to provide shielding to nearby electronic devices due to the potential for electronic interference. The enclosure for the SCR served to provide shielding. The benefit is a much smoother temperature response compared to relays or zero cross-firing mode SCRs. The sensitivity of the cooling load measurement to both supply and return temperatures warrants the use of phase angle SCRs over zero cross-firing mode SCRs.

3.3.3.3 Hot Water Reheat

Hot water reheat is provided by a booster coil tied into the leaving water from the heat pump. The benefits of the hot water reheat are that the temperature response is smooth and that the energy source is heat pump "waste" heat. The negatives of hot water reheat are that the temperature response for an increase in reheat is not the same as that for a decrease in reheat. The control parameters may not fit both situations equally well. The other main deficiency of the hot water reheat is that while using the heat pump leaving water as a source the capacity is limited.

The hot water coil using the heat pump leaving water as the heat source was selected for the additional benefit it provides in lowering the amount of heat rejection to the ground loop.

3.3.3.4 Integration of Heat Exchangers

The control strategy is to maximize the use of hot water reheat and therefore minimize electricity usage. During times when the hot water reheat capacity is too low, namely at night during off-peak cooling load conditions, the hot water coil was switched to full

reheat and the electric coil will provide the trim reheat to maintain the space at the desired temperature. During peak cooling load conditions, the hot water coil was used alone to provide reheat as the temperature response is much smoother and the uncertainty in the cooling load measurements was lessened. It should be noted that the heat pumps were sized to very nearly meet the peak cooling load, therefore only one reheat source is necessary during the on-peak periods. At off-peak conditions the cooling load may actually be negative (or in a heating load condition).

Chapter 4

Instrumentation of the Experimental Facility

Two goals dictated the facility instrumentation design. First, that data would be available for comparison of measured cooling loads to those that were calculated by the procedures. The calculations by the cooling load procedures would have two cases, one in which the model would be used with standard assumptions, and a second case where the model would be tuned based upon environmental readings and measurement of building parameters. Additionally, some data would be taken that may not be used directly by the tuned models but that could be used to analyze individual heat transfer modules.

4.1 Building Envelope Instrumentation

The envelopes of the two test facilities were instrumented in several ways in order to measure envelope related heat gains and losses. The parameters measured included temperature and thermal conductivity.

4.1.1 Thermocouples

A thermocouple is a junction of two metals. As the temperature of the junction changes a small voltage (typically measured in microvolts) is produced. Sensitive electronic equipment is able to measure this voltage. Tables exist for standard types of thermocouples; however it is wise to calibrate the thermocouples against known temperatures if the range of temperature measurements is small or if the engineering

calculations are shown to be sensitive to accurate temperature measurements. Calculations involving a "small" temperature difference, such as cooling loads determined by air mass flow and the change in temperature across the supply and return, require very accurate temperature measurements.

"Type T" thermocouples are often used in building thermal science experiments as their voltage response as a function of temperature is approximately linear in the range of temperatures normally encountered in building heat transfer experiments. This project used Type T thermocouples.

Fluke dataloggers were used to measure the voltages of the thermocouples and convert to engineering units of temperature. Calibration data was used to correct for inaccuracies in the thermocouple construction. Calibration was performed in software.

4.1.2 Solar Radiation

Solar radiation measurements were taken at the facility to collect more accurate data that could be used as input to the procedures. Measurements taken include:

- incident solar (using pyronometers mounted on the side of the building as well as pyronometers on the MesoNet station)
- surface absorptivities/reflectivities (using the net radiometer)

The measured solar data can be used in several ways. They may be compared to the data calculated by the ASHRAE Clear Sky Model and other solar radiation models. The measured solar data can also be used to show the uncertainty in a cooling load due to

using the modeled solar radiation values instead of measured data. This is called a "tuned model".

4.1.3 Thermal conductivity

The equivalent thermal conductivity of the wall constructions was measured using the guarded hot-box method. During construction of the facility wall sections for each test cell, smaller sections made of the same wall construction and same batch of materials were constructed such that a known heat flux could be applied to the wall section and measured using a specially constructed experimental apparatus. Known overall heat transfer coefficients for the wall constructions eliminates error associated with the differences between as-built building surfaces and table lookup data. Uncertainty due to different material properties was eliminated by constructing the test sections from the same batches of materials and by the same technicians. Both test facilities utilized components that are mixed on site as they are used in the construction. The heavy test cell had significant amounts of concrete which could vary depending on the mason who mixed it. The light test cell had a stucco type coating that also must be mixed on-site.

Test wall sections were created to measure the wall properties. The hot-box analysis was completed as part of a Senior Capstone Design project in the Mechanical and Aerospace Engineering Department. The results of the hot-box testing were incorporated into the procedure validation papers. The measured effective conductivity for the light building wall section was 0.203 Btu/(°F·ft2·h) compared to a table lookup value of 0.200

Btu/(°F·ft2·h). The solid masonry wall construction was not measured in the guarded hotbox.

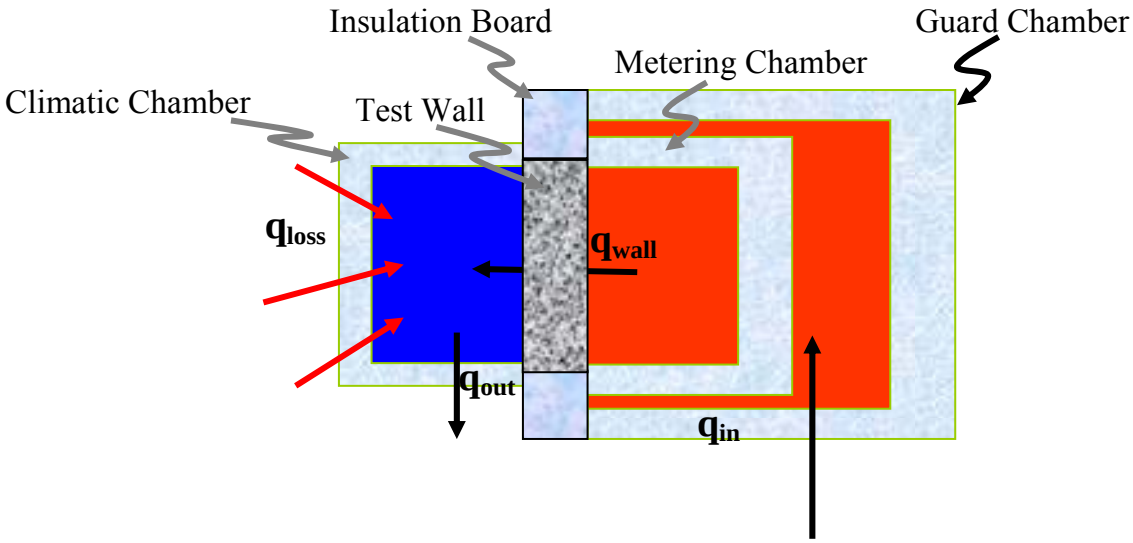

Figure 4-1 Guarded hot box schematic

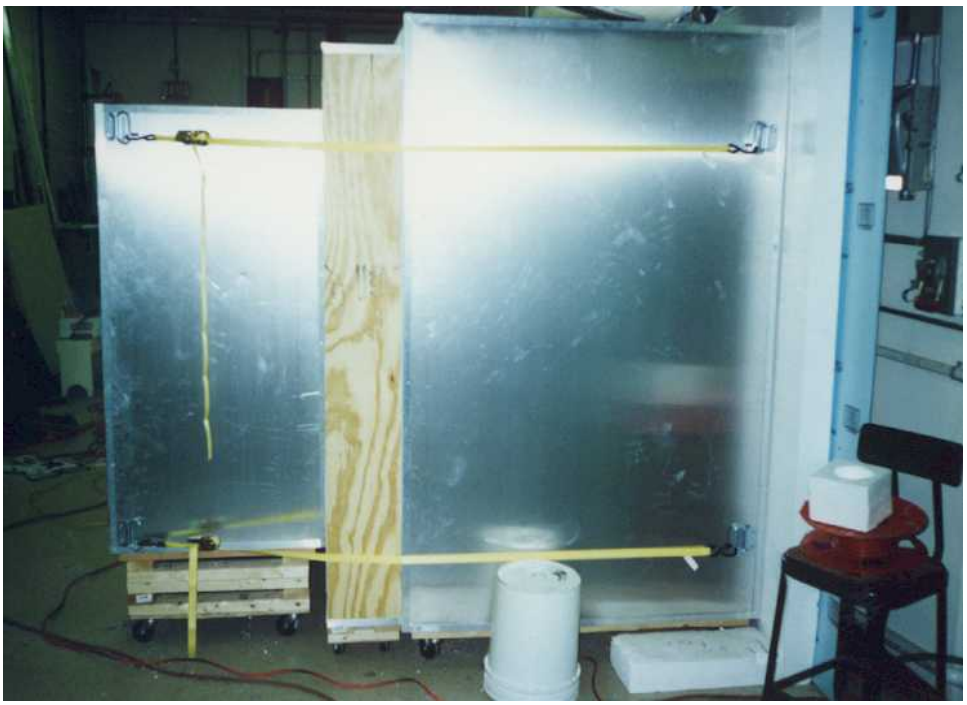

Picture 4-1 Guarded hot box

4.2 Building System Instrumentation

4.2.1 Air Mass Flow

The air mass flow rate is measured according to ASHRAE standard 51. The air leaving the heat pump passes through a settling means and then proceeds through an elliptical flow nozzle. A second smaller settling means is included after the nozzle. The pressure drop across the nozzle is measured and this gives a volumetric flow rate. Air density can be related to its temperature and humidity ratio. Combining volumetric flow rate and density we can find the mass flow rate.

The nozzle selected was a 5" throat diameter nozzle with (L/D) = 0.6. The nozzle was ordered from a machining company that produces AMCA standard elliptical nozzles. The nozzle and pressure tap specifications were taken from the ASHRAE standard. (ASHRAE 1975.)

The size of the ducting was constrained by the space available and also by the nozzle selection. The goal was to make the smallest possible chamber for the largest useable nozzle. 18 inches square cross-section was chosen according to the standard.

A flow chamber diagram can be seen in Figure 4-2. The flow chamber was then constructed from four 18" x 18" x 18" duct sections. The first section connects to an elbow coming from the heat pump blower. There is a settling means located after this first section, consisting of three meshes of increasing percent mesh. The meshes are 60% open, 50% open, and 45% open and are located one inch apart. These are in accordance

with ASHRAE Standard 51. The second section has pressure taps attached to it near the nozzle as proscribed in the ASHRAE standard. The nozzle is next, fastened with epoxy glue to a plate that bolts between duct sections. The next duct section is identical to the previous one except turned so the pressure taps are again near to the nozzle. The last section of ducting makes a 90° elbow to send the air up through the supply duct. Also there is a transition/reduction from 18 inches square cross section to 12 inches square cross section. A second settling means is located between the last two rectangular duct sections.

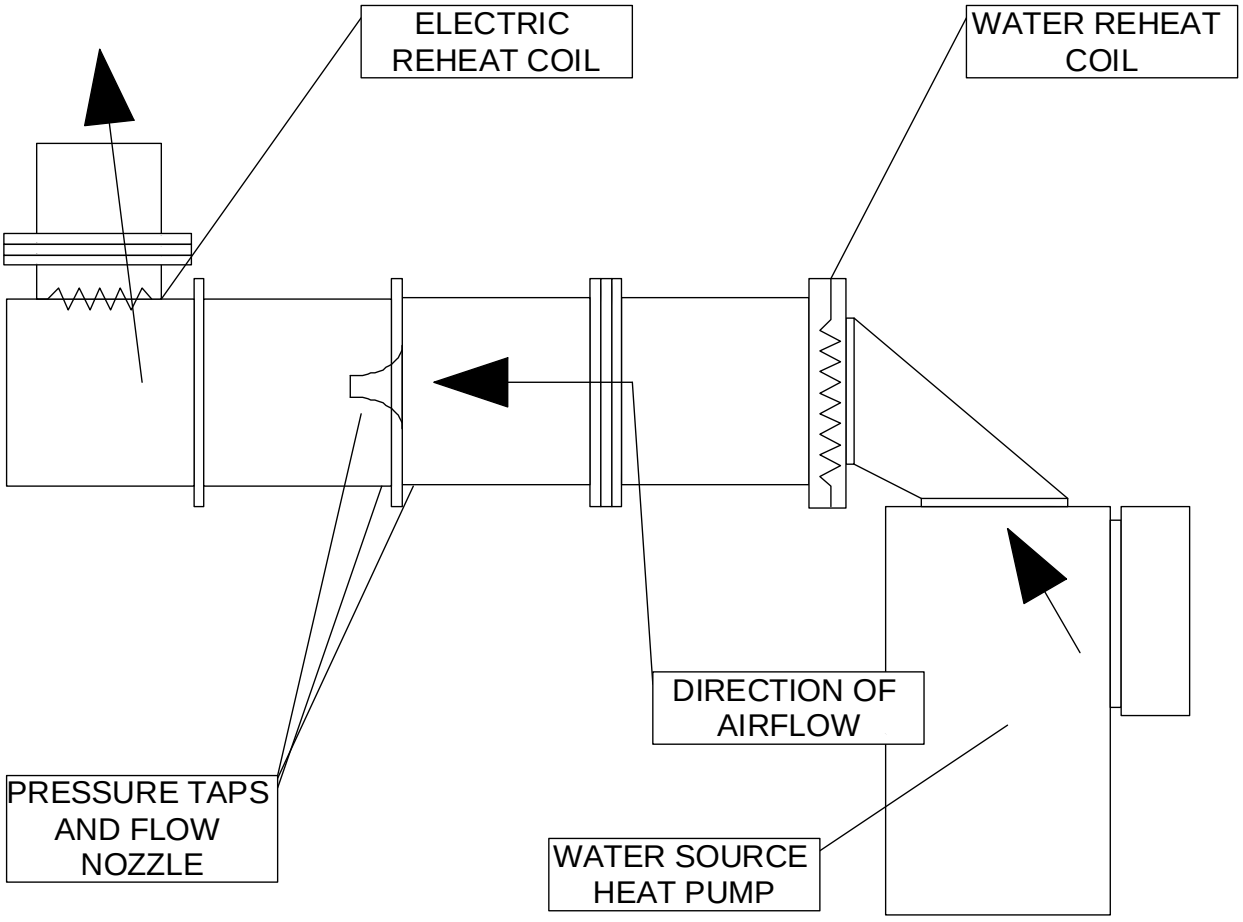

Figure 4-2 Diagram of measurement section assembly with heat pump and reheat coils

Weather stripping is placed between any two mating metal surfaces in the duct assembly to minimize air leakage. The interfaces are all taped and/or caulked after the final setup is determined in order to fully minimize the air leakage. Figure 4-2 above shows the measurement chamber as it was actually constructed.

4.2.1.1 Pressure transducers

The pressure transducers were ordered from Setra corporation. The model selected was the model 264 differential pressure transducer. They output 0 to 5 VDC proportional to 0 to 2.5 inches of water. There is a slight zero offset that can be either adjusted on the transducer or accounted for in software. Their accuracy is +/- 1% full scale. The pressure transducers are attached to a manifold system so that the four pressure taps on one side of the nozzle are mechanically averaged and connected to the transducer.

4.2.1.2 Nozzle

The flow nozzle was ordered from Helander Metal Spinning Corporation. They produce standard nozzle sizes according to AMCA standards. Two five inch nozzles were ordered, as well as a four inch nozzle. The four inch nozzle generates a larger pressure drop that could be beneficial in certain experimental conditions. Generally speaking the five inch nozzle will be used for the current building tests as the pressure drop is a reasonable value according to industry practice while maintaining desirable system airflow. Past experiments have shown that a pressure drop of at least one-half inch of water column gives good results.

The nozzle is glued to a flat plate that is bolted into the duct assembly. Gluing was chosen to minimize the chances of any air leakage. Past experiments have also used screws to attach the nozzle, although this would also require the use of some sort of sealant.

4.2.1.3 Settling Means

The settling means are constructed from three different mesh screens, of 60%, 50%, and 45% open area. The screen was ordered from Southwestern Wire Cloth Company. The screens are placed between square rings made from one inch square channel iron. The channel iron acts as a spacer, the one inch size channel iron matches the ASHRAE standard spacing between screens. The settling means assembly must be caulked after installation to keep air from leaking out.

4.2.1.4 Thermocouples

Thermocouples were made as necessary from a stock of 30 gauge type T Teflon coated wire. The thermocouples must be calibrated to account for inconsistencies in the welding process. Thermocouples provide an accurate measurement of airflow temperature when one of two conditions is met: if the air is uniform temperature, or if the velocity profile is uniform. These two conditions rarely are met, however as long as care is taken to place the thermocouples in a position that these conditions are approximated the measurements are considered reliable. Type T thermocouples are used in HVAC experiments due to their excellent approximation to a linear function for temperature ranges seen in building applications. Type T thermocouples consist of a copper wire and a constantan wire. Small gauge wire is used (mostly 30 gauge) so that the temperature response of the

thermocouple will be fast. Larger wire (and therefore thermocouple beads) have the benefit of being more durable, however the increased maintenance of the small gauge wire is more than offset by the nearly instantaneous change in temperature (and therefore the associated electrical response) of the thermocouple.

4.2.1.5 Supply Air Temperature

A thermocouple grid arranged in the circular duct measures the supply air temperature. Thermocouples are placed at three radii, four at a distance about 4" from the center, four at a distance about 2" from the center, and one thermocouple at the center. The diameter of the duct is ten inches. More accurate and steady measurements are taken if the measurement plane is farther upstream from any transitions or instruments. Therefore, the measurement plane for the supply air temperature is placed four feet into the room, inside the ducting that carries the supply air to the diffuser. The ducting is insulated with R-18 batt-type insulation so that the room control volume in effect excludes the supply air duct up to the location of the measurement plane.

4.2.1.6 Return Air Temperature

The return air temperature is measured similarly to the supply air temperature. The duct for the return air is 12 inches in diameter. The lower thermocouple density is appropriate as the return air temperature approximates the room temperature of a well-stirred thermal zone, therefore less deviation is expected. The well stirred assumption must be verified by experimental instrumentation separately from the thermocouples.

4.2.2 Water Mass Flow

Water loop mass flow rate is measured using an Omega volumetric flow transducer connected in line with the water coming from the ground. Mass flow can be determined from the density of the water at the supply temperature and the volumetric flow. The density of water over the range of operating conditions can be assumed constant.

4.2.3 Water Temperatures

Water loop temperatures are measured at the inlet and outlet to the heat pump by thermocouples. These thermocouples are of the probe variety and are ordered from Omega Corporation and were not welded in the laboratory.

4.3 Instrument Calibration Procedures

Experimental results depend upon calibration of the instruments used to record data. Various calibration procedures were used in conducting this experiment.

4.3.1 Thermocouple Calibration

Calibration of thermocouples is necessary due to inconsistencies in the thermocouples' construction. Imperfect welding and damage to the lead wire can cause small changed in the voltage that is generated by the temperature at the thermocouple's bead.

Thermocouples were calibrated using three temperature points. Any three temperatures spanning the range of temperatures encountered in the experiment will suffice; practical temperatures that were used were freezing, room temperature and "warm". The ice bath temperature is used due to the impending phase change of water at that temperature. A

special ice-bath thermometer was used to measure the actual temperature of the water and compared to the temperature measured by the thermocouples. This process was repeated for a room temperature bath and also a warm temperature bath.

Once three data points for a thermocouple are determined, the measured temperature can be corrected to the calibration points. Once a thermocouple is calibrated, it should not be removed from the sensing device or altered if at all possible.

4.3.2 Pressure Sensor Calibration

The Setra pressure transducers are calibrated in two steps. First, the output of the sensor is adjusted to be zero by adjusting the zero pressure output when no measurements are being taken. The second adjustment is to adjust the span when a reading is being taken compared to the reading shown on a water manometer.

4.4 Data Acquisition

The data acquisition instruments were Fluke NetDAQ dataloggers. These instruments are very accurate and versatile, as shown in Table 4-1. The Fluke/NetDAQ Cold Junction Compensation (CJC) for thermocouples is excellent, and is a requirement for an experiment to use a large number of thermocouples. The fluke method is to provide CJC, while at the same time providing an isothermal connection box so that the reference end of the thermocouples are approximately the same temperature for all thermocouples. CJC attempts to normalize all of the thermocouples to the same conditions so that measurements between thermocouples can be compared. If CJC is not utilized, identical air stream temperatures for two thermocouples might not have the same electrical

response due to different temperatures at the point of connection to the signal processing equipment.

Parameter	Range	Resolution	Accuracy
DC Volts	90 mV to 150 V	0.3 μV to 1 mV	0.01%
AC Volts	300 mV to 30 V	10 μV to 10 mV	0.3%
Resistance	300 O to 3 MO	1 mO to 10 O	0.015%
Thermocouple (Type T)	-100 C to 400 C	0.02 C	0.3 C

Table 4-1 Fluke NetDAQ 2640 resolution and accuracy

The Fluke 2640 NetDAQ dataloggers accept 20 analog inputs and also have 10 computed channels, where simple operations can be performed on the analog channels and/or the other computed channels to get engineering quantities. The 2640 NetDAQ can scan as fast as 100 channels per second, however accuracy is reduced. For HVAC experiments where measurements are taken every minute or longer time period, the Fluke is best used in slow mode where it can scan 6 channels per second. The 2640 NetDAQ has an 18 bit analog to digital converter.

Chapter 5

Experimental Procedure

The following sections will provide details about the experimental procedures used to acquire the data and calculate cooling loads from the measured data and then compare those calculations to modeled data from the cooling load calculation methods based upon the experimental conditions.

5.1 Calculation of Cooling Loads from Measured Data

The first step in the experimental procedure is to calculate the measured cooling load based upon the data collected according to Chapter 4 of this thesis.

The instantaneous cooling load is determined at steady-state conditions by Equation **(5-1)**.

$$q = \dot{m}_{air} \times c_p \left(T_{return} - T_{supply} \right) \tag{5-1}$$

Where:

q	=	Cooling load	btu/hr
$\dot{m}_{air}$	=	Air mass flow rate	lbm/hr
c_p	=	Specific heat of air	btu/lbm·°F

T_{return}	=	Air temperature leaving the zone	°F
T_{supply}	=	Air temperature entering the zone	°F

The ASHRAE standards allow us to calculate the mass flow of the air according to equation

$$Q = 1096 \times Y \times \sqrt{\frac{\Delta P}{\rho}} \times \left(C \times A_{exit}\right) \tag{5-2}$$

Where

Q	=	volumetric flow rate	CFM
Y	=	Nozzle expansion factor	-
ΔP	=	differential pressure across flow nozzle	Inches W.C.
ρ	=	density of air at the nozzle bell	lbm/ft^3
C	=	Nozzle discharge coefficient	-
A_{exit}	=	nozzle throat area	in^2

The expansion factor is calculated from

$$Y = 1 - \left(0.548 + 0.71\beta^4\right) \times \left(1 - \alpha\right) \tag{5-3}$$

Where:

$$\beta = \frac{D_{exit}}{D_{duct}}$$

$$\alpha = 1 - \frac{5.187\Delta.}{\rho_{duct} \times 53.35 \times \left(t_{dx} + 459.7\right)}$$

With:

β	=	Diameter ratio for nozzles	–
D_{exit}	=	Diameter of nozzle exit	Inches
D_{duct}	=	Diameter of duct	Inches
α	=	Static pressure ratio for nozzles	–
ΔP	=	Pressure differential	Inches w.c.
ρ_{duct}	=	Air density	lbm/ft^3
t_{dx}	=	Dry-bulb temperature	°F

Table 2 of ASHRAE standard 51 can also be used. For the relatively low differential pressures associated with the GT018 heat pump the nozzle expansion factor can be approximated as one for all experiments.

The nozzle discharge coefficient can be found using analytical equations found in ASHRAE standard 51, Section 9.3.2.6.

$$C = .9986 - \left(\frac{7.006}{\sqrt{\mathrm{Re}}}\right) + \frac{134.6}{\mathrm{Re}} \qquad (5\text{-}4)$$

Where:

Re	=	Reynolds number at the nozzle exit	-
C	=	Nozzle discharge coefficient from Eq 5-2	-

In practice the nozzle discharge coefficient must be found iteratively with the calculated volumetric flow rate.

5.2 Procedural Estimation of Cooling Loads

The second phase of the experimental process is to calculate the cooling load as modeled by the cooling load calculation procedures. Both the RTSM and Heat Balance Method were simulated utilizing the ASHRAE Loads Toolkit as the modeling tool. The Loads Toolkit was selected based upon its development as a collection of modules that correspond to the inputs that would be used to measure and model the cooling load of the experimental buildings.

The modules that were developed are based on and have been used in other simulation packages that are widely available. Other simulation frameworks could also have been used; however the familiarity and experience of the research staff relating to the Loads Toolkit provided a significant advantage over any other tools that might have been considered.

Detailed descriptions of the comparison between the measured data and the modeled results are included in Chantrasrisalai et al. (2003) and Iu et al. (2003). Chapter 6 includes additional information on the commissioning of the experimental facility.

5.2.1 Development of Baseline Models

Initially, the models are run using published design data and "standard" assumptions for material properties. These experiments are intended to provide insight into the design

process where measured inputs are not available. It is expected that the comparisons will vary slightly from the measured cooling load; however for the Stillwater, OK, location reasonable comparisons should result

These baseline experiments are not necessarily suitable for validation of the cooling load methods at a high level, but are useful to show some of the effects of standard design assumptions that may be used in design practice and how the results may vary based on the unpredictability of construction.

5.2.2 Tuning the Baseline Models

The models are also run using the actual measured thermophysical parameters and measured weather data that occurred during the experiments. This allows a much finer comparison between the measured cooling load and the modeled values. The models were tuned based upon:

- Measured temperatures
- Measured solar radiation
- Wind velocity (direction and speed)
- Internal surface absorptances
- External surface absorptances

Other parameters were equivalent between the baseline model and tuned models.

Chapter 6

Validation of Experimental Facility

The facility as a whole and several subsystems of the testing apparatus were put through separate experiments to validate their capability to take accurate and meaningful experimental data. These tests included heat balance calculations in the laboratory along with efforts to quantify or eliminate experimental inputs that could result in uncertainty in the final calculations.

6.1 Air Flow Measurement System

In order to verify the accuracy of the flow measurement box, the system was subjected to a laboratory heat balance test prior to installation in the test cells. A large, nearly adiabatic chamber was constructed in the laboratory. An electric heating element consisting of three 11 Ohm coils provided a constant, measurable source of energy to the chamber. Resistance levels were measured using the Fluke™ dataloggers. The coils were wired to allow any combination of the three coils to be switched on. The chamber had a long section of insulated ductwork with a series of baffles and mesh screens at the exit to allow the air to mix after passing over the heating coils. The load section was attached to the heat pump and flow measurement section as shown in Figure 6-1. Photographs of the laboratory setup are included in Picture 6-1. Calibrated thermocouple grids were located upstream and downstream of the heating chamber as shown in the figure.

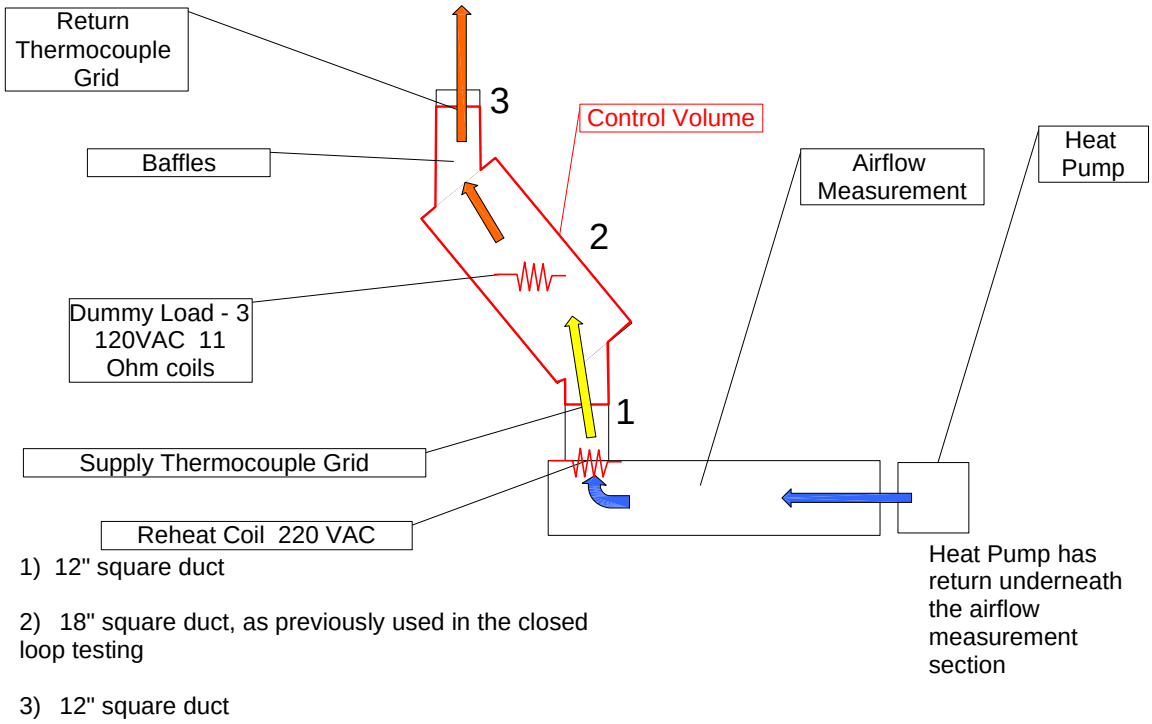

Figure 6-1 Instrumentation commissioning diagram

Picture 6-1 Laboratory setup for instrumentation commissioning photographs

The heat balance tests were performed by manually switching the power input to the electric heating coil. The electric power input was calculated from the measured coil resistance and the measured line voltage. The heat extraction rate, which at steady state should equal the heat addition rate, was calculated from the measured temperatures and volumetric air flow rates as shown in Equation **(5-1)**.

The results of the laboratory heat balance tests in Figure 6-2 show that the air flow and temperature measurement systems are accurate to within ±5% for steady or slowly changing cooling loads. This value is well within the calculated uncertainty of ±7.4% derived in Chapter 7.

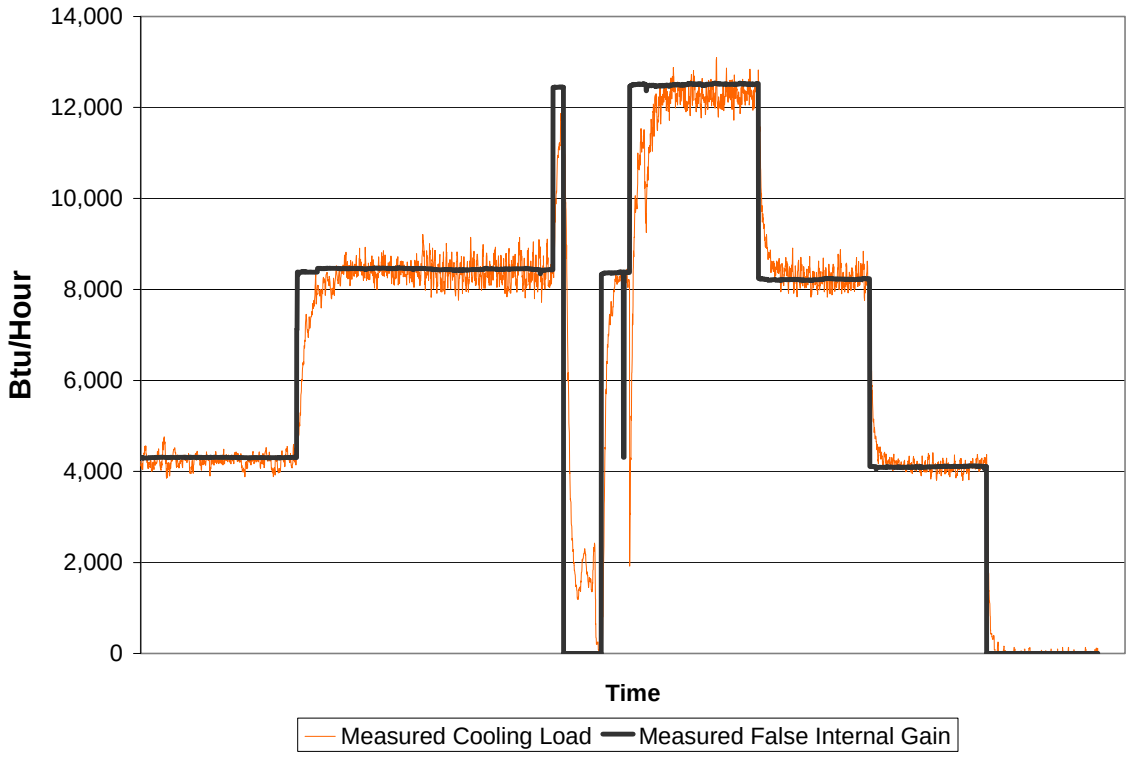

Figure 6-2 Instrumentation commissioning results

6.2 Infiltration

The infiltration rate into the buildings is very important to the reconciliation of the simulated results to the experimental results. It is a quantity that is difficult to measure

and model. It was intended in the ASHRAE project design to build the structures 100% airtight, such that infiltration could be modeled as a zero quantity; however construction constraints prevented this from happening. Such that there is some infiltration, some estimate of that infiltration rate must be accounted for in the computer simulations if the experimental and theoretical results are to be compared. For an infiltration rate of 10 cubic feet per minute (CFM) and an inside/outside temperature difference of 10 °F the result would be 100 Btu/h difference between measured cooling load and simulated cooling load. This contribution to the heat gain could clearly be quite significant for large ΔT or high infiltration rates.

6.2.1 Methodology

The pulse and decay method was used to estimate the infiltration flow rate. Carbon Dioxide was released in the structures and the concentration was measured as it was replaced by air from outside the structure. A simple analytical model was then formulated based upon a control volume mass balance and fit to the experimental data.

6.2.1.1 Experimental Apparatus - Buildings

Both buildings were intended to be very tight, allowing the simulation to assume negligible infiltration. Actual conditions showed that the construction was not to the desired quality level and the buildings leaked considerably.

6.2.1.2 Experimental Apparatus - CO_2 Sensor

The CO_2 sensor outputs a 0 to 4 VDC signal proportional to measured concentrations of 0 to 4000 ppm. The response of the sensor is stated as < 1 minute for a 90% step change.

The speed of measurement is more than adequate for the research purposes. The readout on the sensor goes from 0 to 9999 ppm. A suggested improvement to the sensor might be to increase the analog output to match the readout range. It should be noted that in an actual building 4000 ppm is much larger than desired levels and would signal the need for immediate action. In our case where the CO_2 is the important quantity being measured and not just a companion gas for more toxic molecules the useful range could be larger.

6.2.1.3 Experimental Apparatus Fluke Datalogger

Measurements were made by Fluke™ NetDAQ dataloggers. The NetDAQ series are the most technologically advanced dataloggers available. They communicate over an Ethernet network and can measure DC Voltage to +/- 0.01%. Measurements on the order of 5 seconds to 5 minutes are useful to this experiment. The fluke can measure 6 channels per second in its most accurate mode of operation; this is more than sufficient for our purposes.

6.2.1.4 Pulse and Decay Method

The pulse and decay method was chosen as the method to use for this project. It provided necessary accuracy for a small test cell, and also required the least amount of equipment and other overhead.

The first step in starting an experiment was to take dry ice to the test cell. Dry ice is solid CO_2, and is a convenient method of handling the CO_2. The dry ice is then smashed into a powder on the test cell floor. This is very important, for the simplified analytical

equation to work there is assumed to be no source term – there simply is a pre-existing concentration. If the dry ice is dissipating over time the result will not be the same. Alternatively, the dry ice could be placed on a scale and weighed, and the actual sublimation calculated. This introduces several degrees of difficulty however, and was not necessary for this experiment.

Enough dry ice is smashed to raise the concentration in the room to a level moderately above the range of the analog output. This allows the experimenter some error in exiting the facility, and also a short grace period for the dry ice to fully sublimate.

After the concentration readings in the room are satisfactorily high, the door is locked and sealed and the datalogger is started if it is not already. Anomalies in the data at this point as the data will be "chopped off" at the point where the datalogger starts showing changes in the concentration. Typically this might be 30 minutes to an hour. Reasonable amounts of dry ice used were determined by trial and error.

6.2.1.5 Analytical Model

There is an analytical solution to the infiltration problem. A few assumptions need to be met to make the problem tractable however. First, the infiltration rate must be assumed to be a constant over the modeled time step. Next, the infiltration must be assumed to be between two nodes, one node that is assumed to be well stirred (the room) and the other that should be assumed to be constant. Making these assumptions, we are able to get a solution in one variable subject to one set of initial conditions. Due to the nature of the

CO_2 sensor, the majority of the infiltration test runs will also have the same initial concentration of 4080 ppm.

Setting up a mass balance on the test cell volume we get the Equation (6-1)

$$Q\frac{dC_{room}}{dt} = \dot{q}_{\inf}(C_{room} - C_{OA}) \quad \textbf{(6-1)}$$

Where:

Q = volume of the room	ft^3
C_{room} = concentration in the room	ppm
q_{inf} = infiltration rate into the space	ft^3/sec
C_{OA} = concentration of the environment	ppm
d/dt = rate of change	1/sec

Solving the differential equation gives Equation (6-2)

$$C(t) = C_1 + C_3 e^{-C_2 * t} \quad \textbf{(6-2)}$$

Where:

C(t) = concentration of the room as a function of time

C_1 = condition at time $t = \infty$

C_3 = constant of integration, solved with the initial condition time t = 0

C_2 = constant related to the infiltration rate

C_2 can be calculated based upon the infiltration rate and the volume of the room, as seen in Table 6-1.

ACH	CFM	C_2
1	24	1/3600
0.75	18	1/4800
0.5	12	1/7200
0.25	6	1/14400
0.125	3	1/28800

Table 6-1 C_2 coefficients for solution of Equation (6-2)

6.2.2 Results

Many iterations of the testing took place before the final data used was taken. Many of the early data were taken only to find that much work remained in tightening up the two buildings.

6.2.2.1 Heavy Building

The two main sources of infiltration were different for each building. In the heavy building the major source of infiltration was the framing around the windows and door. Attempts to seal these areas had been undertaken several times, however it appears that there will always be one or two more places to apply some caulk. The first pass was around the windows as they were clearly not airtight. The next round focused on the

framing around the windows. The last infiltration was found on the door framing. The current status of the infiltration is reasonable for a still day, as shown below in Figure 6-3. The dark blue data in Figure 6-3 is the measured data. The thin red and blue lines show the analytical solution for 0.25 ACH and 0.125 ACH. The thin purple line shows the analytical solution for 0.50 ACH. The infiltration rate is not determined exactly, but it is between those two values, approximately 0.188 of an air change per hour on days with average wind speed of 9 mph. The infiltration rate was approximately 0.50 ACH on the day with average wind speed of 17 mph.

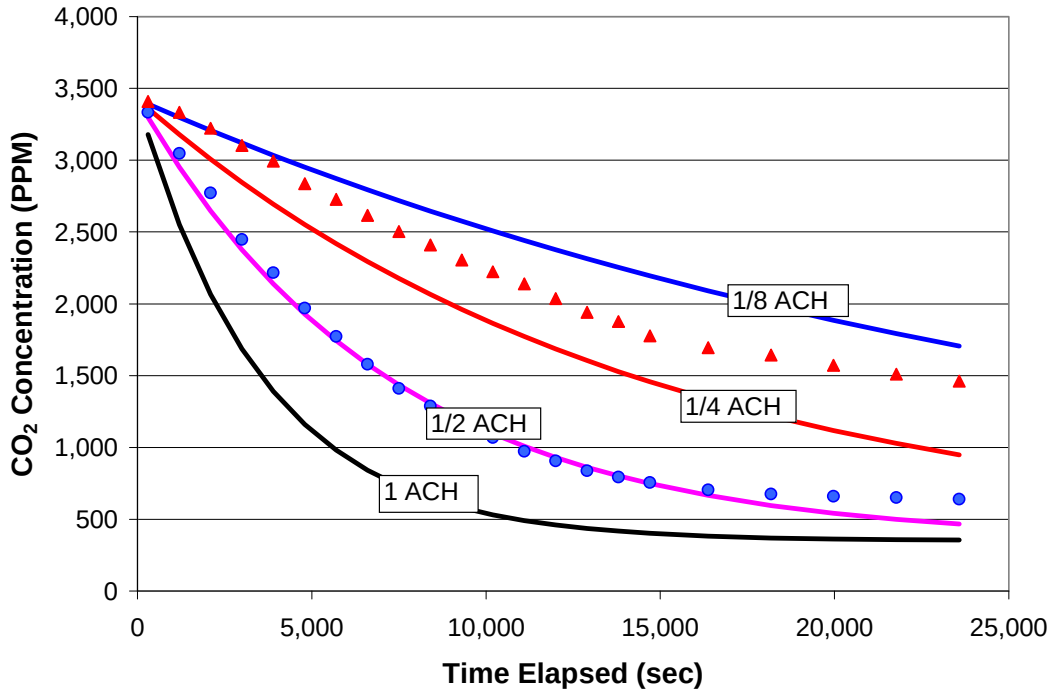

Figure 6-3 Heavy building infiltration for two days with varying wind speeds

6.2.2.2 Light Building

The light building infiltration was characterized by a different mechanism. The building envelope was quite airtight, as it is a plastered surface similar to stucco. A little caulk

around the windows and the walls are completely air tight. However, due to the layering of the wall constructions a path existed for air to flow around the edge of the floor slab from the control room. This was determined to be the case by releasing a CO_2 charge in the control room while the test cell was initially at the environmental concentration. The concentration in the room rose quickly to many hundred ppm. A bead of caulk was then applied to the base of the wall around the floor slab to reduce this infiltration. A subsequent test, shown in Figure 6-4, showed much improvement in the infiltration rate.

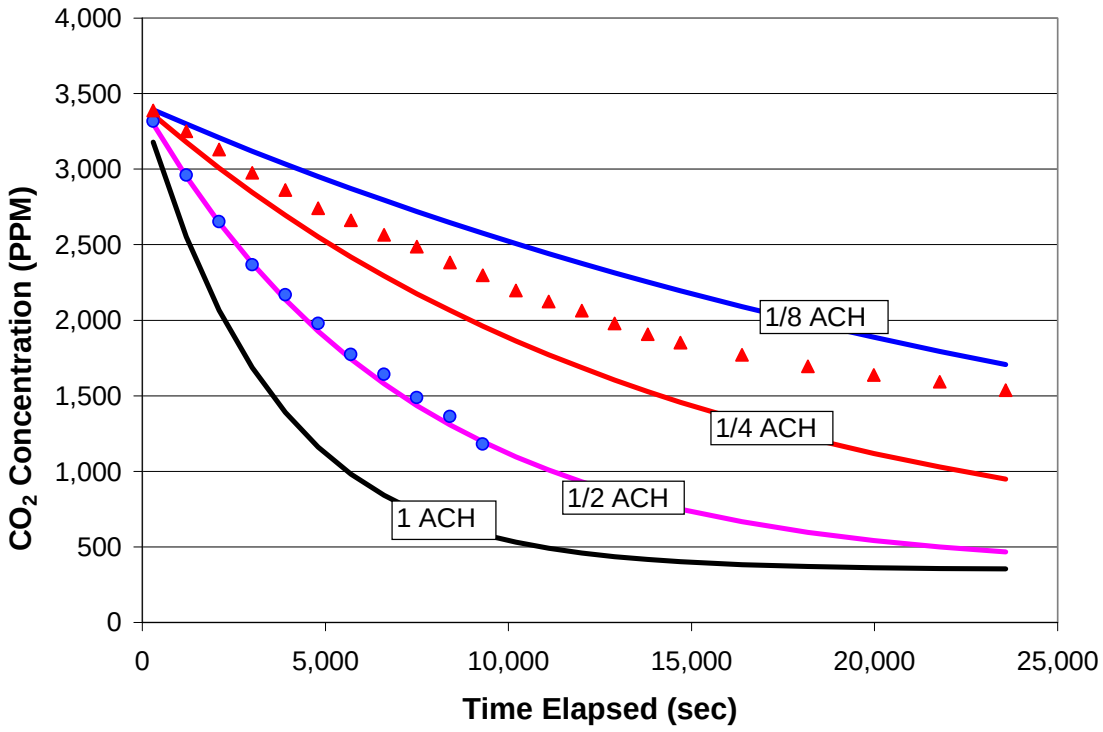

Figure 6-4 Light building infiltration for two days with varying wind speeds

The thin red, purple, and blue lines represent analytical solutions for several infiltration rates. Clearly the result lies between 0.25 ACH and 0.125 ACH, and furthermore 0.188 ACH is a close match to the experimental data. The existence of just the one data set

would preclude us from stating that the infiltration rate actually is equal to 0.188 ACH, but we do have reason to expect to be close to that as shown Figure 6-4.

The light building results then are determined to be very sensitive to the status of the control room – especially if the door is left open. Further study is needed to more accurately determine the infiltration of this building. For the time being, it is sufficient to say that the infiltration is "small" as long as care is taken to secure the control room during testing and that average wind speeds are less than 10 mph.

6.2.2.3 Model Inputs

Once the buildings were tightened up to minimize air leakage, a single infiltration value could be used to describe both buildings. A value of 0.19 ACH with an error range of 0.125 ACH was selected for low windspeeds (9 mph) and a value of 0.5 ACH with an error range of 0.125 ACH was selected for high windspeeds (17 mph) as shown in Table 6.2

	Low Wind Speeds	**High Wind Speeds**
Infiltration Rate	0.19 ACH	0.5 ACH
Error Range	0.125 ACH	0.125 ACH

Table 6-2 Infiltration results for experimentation

Chapter 7

Uncertainty Analysis in Cooling Load Calculations

7.1 Experimental Uncertainty

Validation of the cooling load procedures required that both the uncertainty associated with measured data and the uncertainty associated with model inputs be quantified. The experimental uncertainty was calculated by the method, proposed by Kline and McClintock (1953), of adding the component errors in quadrature. The uncertainty associated with model inputs (such as material thermal properties, boundary conditions, and infiltration rates) was arrived at by the method of influence coefficients and is discussed in a companion paper (Chantrasrisalai et al. 2003).

The experimental uncertainty associated with the cooling load calculated from Equation **(7-1)** can be written as:

$$e'_Q = \pm\sqrt{e'^{\,2}_{\dot{V}_{air}} + e'^{\,2}_{\Delta T} + e'^{\,2}_{\rho} + e'^{\,2}_{Cp}} \tag{7-1}$$

The total experimental uncertainty is dependent on the uncertainty associated with each term in the cooling load equation.

The first term in Equation **(7-1)** represents the uncertainty associated with the volumetric flow rate. ASHRAE standard 51, which specifies the air flow measurement system, includes a detailed uncertainty analysis. The following relationship is given for the fractional uncertainty in the volumetric flow rate:

$$e'\dot{v}_{air} = \pm\sqrt{e_c^2 + e_a^2 + e_{fs}^2 + e_{\Delta p}^2 + e_{sp}^2} \tag{7-2}$$

where:

$e'\dot{v}_{air}$ = uncertainty in the volumetric flow rate

e_c = fractional error in the nozzle discharge coefficient

e_a = fractional error in the nozzle area

e_{fs} = fractional variation in fan speed

$e_{\Delta p}$ = fractional error in pressure difference across flow nozzles

e_{sp} = fractional error in static pressure

The standard provides the following typical uncertainties for the nozzle discharge coefficient and the nozzle area:

$$e_c \tilde{} \pm 0.012$$

$$e_a \tilde{} \pm 0.005$$

The constant speed fans are accurate to within ±1% ($e_{fs} = \pm 0.01$), and since the static and differential pressures are never allowed to drop below ˜0.2 inches WG, the maximum fractional error in the pressure measurements as specified by Setra, is ±1%, ($e_{\Delta p} = e_{sp} = \pm 0.01$)

This results in a total fractional uncertainty in the volumetric air flow measurement of ±0.02 such that :

$$e'_{\dot{V}_{air}} = \pm 2\% \tag{7-3}$$

The second term in Equation **(7-1)** represents the uncertainty associated with the temperature difference between the room air inlet and outlet. The uncertainty in the spatially averaged inlet and outlet temperatures is estimated to be ±0.5 °C
Thus the uncertainty in the temperature difference is:

$$e'_{\Delta T} = \sqrt{0.5^2 + 0.5^2} \approx \pm 0.71\,^{\circ}\mathrm{C} \tag{7-4}$$

The last two terms in Equation **(7-1)** represent the uncertainty due to errors in estimating the density and the specific heat of air. Since both density and specific heat are calculated as functions of the measured air temperature, the uncertainty associated with these variables is small. The specific heat of air varies by less than 0.2% over the entire range of experimental conditions. Although the density of air varies by 16% over the

same range, the uncertainty in this property is due primarily to the uncertainty in the measured air temperature (±0.5 °C). Under typical conditions, this amounts to less than 5% and translates into a density uncertainty of less than ±0.1%. Since the uncertainties associated with the volumetric flow rate and temperature are an order of magnitude larger, uncertainties associated with property calculations can be neglected.

The fractional uncertainty of cooling load is therefore calculated as:

$$e_Q = \sqrt{e_{\dot{V}}^2 + \left(\frac{e_{\Delta T}}{\Delta T}\right)^2} \tag{7-5}$$

or

Error! Objects cannot be created from editing field codes. (7-6)

For a 10 °C temperature difference, the uncertainty of the measured cooling load would be about ±7.4%.

7.2 Modeling Uncertainty

The results are also subject to uncertainty due to the model inputs. The test cells were designed to minimize or eliminate these effects wherever possible, however they cannot be completely eliminated. Chantrasrisalai et al. (2003) covers the magnitude of these uncertainties in the Heat Balance Method Validation.

The scope of this project was to design the facility such that uncertainty (due to any cause) would be minimized such as using the simplest glazing, measured conductivities, measured infiltration rates, etc.

In practice many of the modeling inputs will be estimated. The typical building will be designed with other purposes at the forefront rather than providing for accurate cooling load calculation – the load calculations must adjust to the proposed building instead. This potential area of conflict is suggested as a topic of future research.

Chapter 8

Facility Operation and Performance

In order to maintain a constant room temperature, the heat pump compressor operated 100% of the time. A combination of electric and hot water reheat tempered the supply air in order to maintain a constant return air temperature. Temperatures were measured by thermocouple grids placed in the supply and return ducts. The return air thermocouple grid was located in the floor slab. Sunlight was not able to fall directly on the thermocouples. The supply air thermocouple grid was located in the vertical ductwork leading to the ceiling diffuser. The ductwork was insulated to prevent heat transfer with the room. Additionally, the supply air thermocouple grid was located far away from the electric reheat coil to eliminate radiation exchange between the two.

The return temperature was typically maintained to +/- 0.25 ˚C during steady periods as shown in Figure 8-1 for the light building and to an even closer tolerance in Figure 8-2 for heavy building. As expected, the supply air temperatures are consistent and vary throughout the day due to reheat.

The temperature controllers are observed to briefly lose control of the building when the sun goes down. This occurs for a short duration during a time of low cooling load transitioning to even lower cooling load, therefore this effect is not considered to be significant.

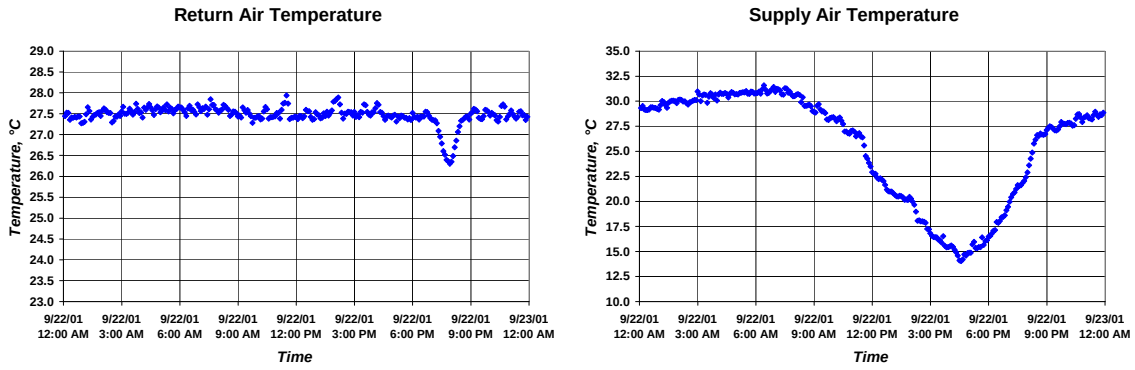

Figure 8-1 Light Building Supply and Return Temperatures

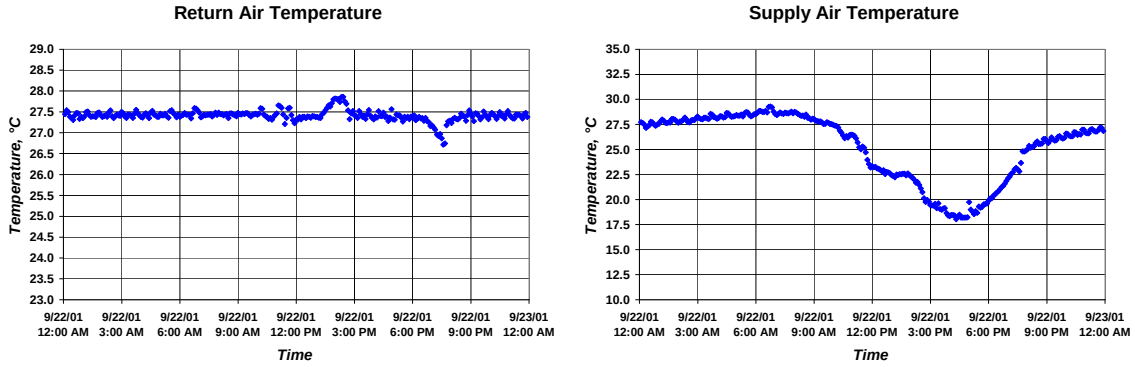

Figure 8-2 Heavy Building Supply and Return Temperatures

The uncertainty bands are affected by the thermocouples, the measuring instruments, and the conditions. Small bead thermocouples were used resulting in small Biot numbers (approximately uniform temperature) giving a fast response. Slower response thermocouples could be used giving a smaller uncertainty band, however control would lag the experimental conditions.

The reheat coils were controlled on the return air temperature. The controller was tuned to maintain stable control under all operating conditions. The water reheat coil is

activated first to provide a constant amount of reheat. The electric reheat serves to provide trim reheat when the reheat demand is low. When the reheat demand exceeds the capacity of the hot water reheat the hot water valve is fully opened and the electric coil makes up all of the difference.

The doors are sealed during testing with caulk and duct tape to prevent infiltration. The control room of the light building is also sealed with duct tape. Tests are run for three days after achieving a constant room temperature to simulate the steady periodic input to the load calculation procedures.

The buildings were designed to have similar U-values to facilitate experimental conditions where thermal mass was the only difference between the two buildings. Although the U-values of the building walls and roofs were not identical, testing showed that the cooling load was not sensitive to small differences in wall and roof conductivity. Adjusting the heavy building wall and roof conductivity to match the light building resulted in insignificant changes in the heavy building hourly cooling loads.

The effect of the building thermal mass is shown in Figure 8-3. The thermal mass of the heavy building damps the peak cooling load by approximately 25%. An interesting result uncovered during experimentation is that the heavy building shows very little lag in the peak cooling load. This is due primarily to the high percentage of glazing on the west and south walls of the building. The single pane glass has a relatively low thermal resistance compared to the walls and roof. The windows therefore dominate the envelope

heat transfer rates. Since the glazing for the two building is identical, the buildings peak at the same time.

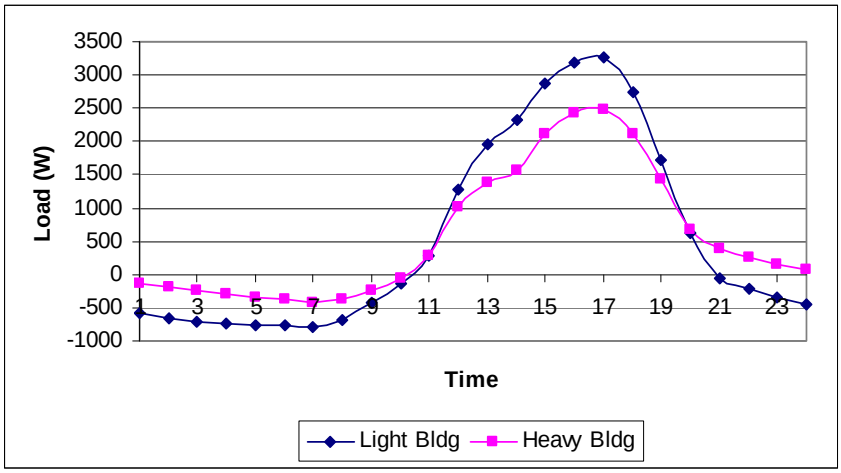

Figure 8-3 Heavy and light building modeled cooling loads

8.1 Sizing

The equipment sizing for the building was determined from a design day run performed with the BLAST program. The design day selected was Stillwater, OK. The construction was not completely known at that time. The block/brick was used; however the second building was originally simulated as a spandrel building. Subsequent design revisions resulted in simulation of the construction to be used, EIFS.

Geothermal heat pumps were selected for the application due to the abundance of heat rejection capacity in place on-site. Each building was outfitted with the next larger size of heat pump from Florida Heat Pump Manufacturing Company. This selection resulted in GT018 models (1-1/2 ton units) being selected to serve the test cell space and GT010

units to serve the control room/guard space. The two units were connected in parallel to two 250' U-tubes.

It was found later that the test cell system configuration exceeded the normal operating range of the factory installed blower. A booster fan was added into the return ductwork. This fan was located downstream of the temperature sensing devices such that fan heat would not affect the calculations.

8.2 Controls

The heat pump runs continuously during testing with a "wild" cooling coil. The two reheat coils are controlled using a programmable logic controller (PLC) that uses a thermocouple grid placed at the same location in the return air grid as the thermocouple grid used to measure the return air temperature. The controller had PID capability which was used to provide as constant of a return air temperature as possible. The controller had the capability of tuning itself depending on the performance of the system it is controlling; this feature was utilized for the operation of the test cells. Typically in HVAC systems the P and I parameters are sufficient to control the building, this was the case for the test cell as well.

The reheat coils are reverse acting. An increase in the measured signal indicates the need for less reheat activation. The return temperature was difficult to control as the building's time constant was very short due to the extremely high rate of air exchange.

8.3 Thermal Mass Characteristics

Initial BLAST runs showed a slight time lag between the peak hours of the two test cells, however the experimental results showed very little lag between the peaks. This is likely due to the overwhelming heat gain from solar loads which peak at the same time for the two buildings. A lower percentage of glazing would allow the lag effect to be more pronounced. Simulation runs on a less than hourly time step might be able to demonstrate this effect.

8.4 Overall Performance

Experiments have been performed under ASHRAE RP-1117. The experiments have shown that the Heat Balance Method and RTSM are able to accurately predict cooling loads, with a few limitations, in several papers. (Iu et al. 2003, Chantrasrisalai et al. 2003.) The Heat Balance Method tracks the experimental results very closely as shown below in Figure 8-4.

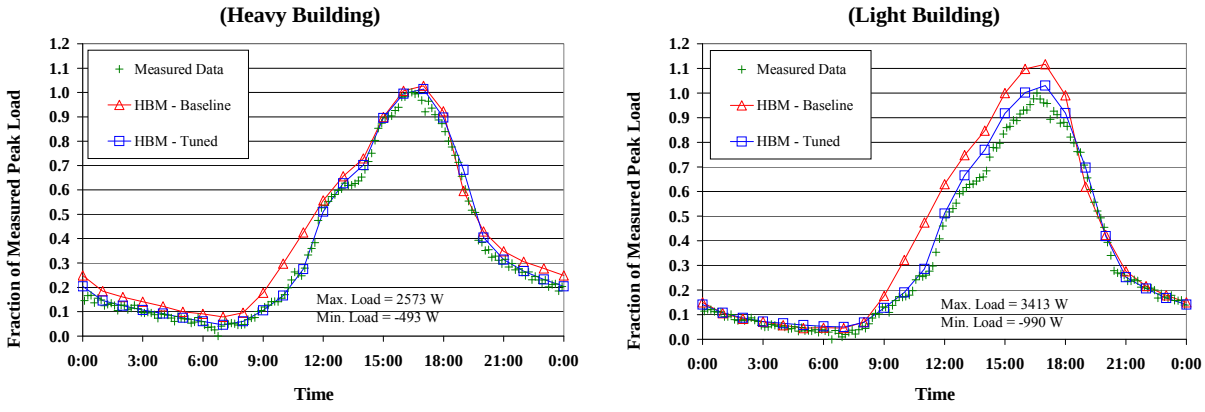

Figure 8-4 Heat Balance Method baseline results (Chantrasrisalai, 2003)

The RTSM results are shown in Figure 8-5. The original version of the RTSM is shown to over-predict the cooling load by approximately 40% for both heavy and light thermal mass test cells. A modified version of the procedure resulted in significantly improved performance as discussed by Iu (2003)

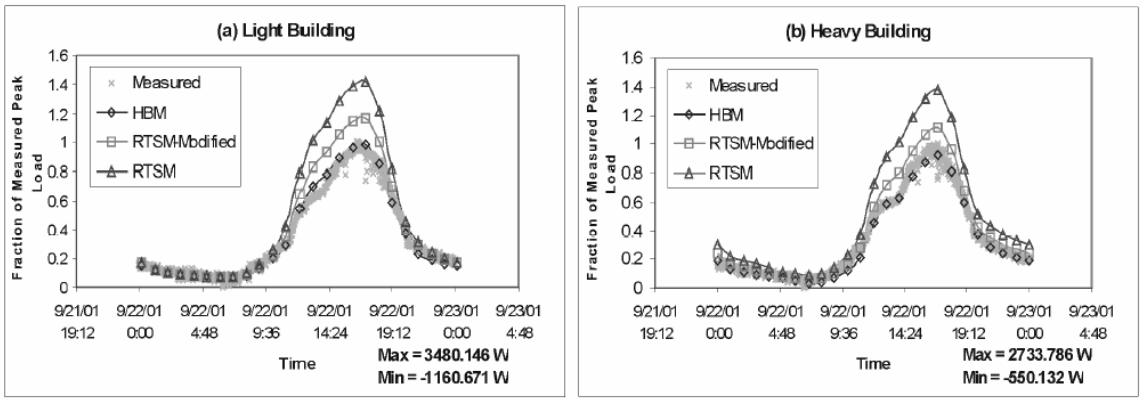

Figure 8-5 Radiant Time Series Method baseline results (Iu, 2003)

The baseline case comparisons suggest that the facility as commissioned is ready to perform validation for the two cooling load procedures.

Example ASHRAE Loads Toolkit model inputs are included for reference in Appendix A. Please note that some inputs specific to the RTSM will be ignored by the Heat Balance Method input processing routines.

Chapter 9

Conclusions and Recommendations

The facility commissioning experiments suggest that the facility will be able to test cooling load calculation procedures spanning a range of construction thermal mass. Additionally testing will be able to be performed to study the influence on cooling load magnitude due to heat gain component models such as interior shading. A wide range of conditions are available for testing at the Stillwater, OK, location. The hot summer days with clear skies are appropriate for testing the Radiant Time Series Method.

Observing the construction and shakedown experiments did provide insight into the experimental process. Future research should consider some of the following ideas:

1. A larger fan with an operating point on the fan curve at a higher CFM and corresponding increase in pressure drop across the nozzle. A larger ΔP measurement reduces the uncertainty in the flow calculation.
2. More thermocouples could be installed in the supply and return air grids. This is an economic limitation – while the thermocouples were relatively inexpensive to make, the datalogging equipment recording their voltages is quite expensive. More thermocouples result in lower uncertainty in the averaging.
3. The electric reheat acts too fast for this size of a closed loop system. Extra time must be spent tuning the controllers in order that the supply temperature doesn't

fluctuate while the controller "hunts" for the desired return air setpoint. A system using only hot water would be easier to control. This would require an additional hot water loop.

4. A larger ground loop should have been installed or a supplemental heat rejection device included in the loop. The heat pump is constantly in cooling mode and the compressor never cycles from spring until late fall (a subset of those hours while experiments are underway). This results in an unbalanced load profile causing the ground loop to gradually increase in temperature over time.
5. Turning vanes should have been installed in the ceiling diffuser to provide more uniform air distribution to the space.
6. Alternative construction methods should be considered. Research staff and hired labor were able to perform most of the construction, however the construction of the filled core concrete block wall consumed a large amount of time, perhaps forms could have been used to pour a solid concrete wall of similar thermal properties to the filled concrete blocks. Savings of time vs money should be compared during the design period.

Equipment selection:

A unit should be selected that has some sort of hot gas bypass in order to provide self-modulation itself. This method of control may not be fine enough for this testing. If hot gas bypass is not utilized due to the constraints, then some form of supplemental heat rejection is necessary due to the non-cycling nature of the system control. Additional loops could be installed at the expense of increased pumping costs. Variable flow

pumps/compressors/fans could be used however this would be highly customized equipment and likely not justified compared to the cost, particularly for units of this size. Also the electric reheat significantly increased the rate of entropy generation in the world. Later in the experimental process the hot water reheat was added utilizing the heat pump outlet water as a first choice for reheat, providing the same effect as a hot gas bypass (that being that the supply air was warmed slightly and the net heat rejected to the water loop was reduced). More reheat strategies of this type should be investigated. The best choice from an energy consumption perspective would be modulating compressor speed, however this might be difficult to arrange on such a small heat pump unit.

An oversized fan should be ordered as well. Using the largest flow nozzle possible due to the space constraints resulted in a pressure drop of 0.62 inches of water column under laboratory testing conditions and 0.41 inches of water column when installed in the field. Additional pressure loss is encountered due to the non-standard ductwork and coils. A slightly oversized fan with modulating capability would have aided the experimentation.

Alternatively a variable flow chilled water system could have been installed that would have reduced or eliminated the need for reheat. Geothermal heat pumps of the water-to-water variety could have been used to fill a common chilled water tank serving coils in both test cells. This may have been the most economical and simple arrangement in terms of equipment and controls.

Construction

Significant expense was incurred constructing the masonry walls of the heavy test cell. If forms were constructed and poured concrete substituted for the filled concrete blocks the labor expenditure (and more than a month of researcher time) could have been saved allowing for additional testing time during the summer. This would be a matter of trading real world construction practices for experimental benefit.

Testing Constraints

At times the closed ground loop showed potential for reaching high temperatures. The range of testing could be extended by replacing the single pane glazing with more robust glazing.

Future research

The ASHRAE load calculation research should be continued to provide information about different architectural configurations for the test cells. The A/E design office has a detailed understanding of the efficiencies of the HVAC equipment. New information regarding carpeting and the effects of blinds or other glazing surfaces would improve the accuracy of load calculations and allow the systems to be designed in the most efficient manner.

The effects of different diffuser locations should also be investigated. Ventilation effectiveness is also a potential hot topic for research.

Chapter 10

Bibliography

ASHRAE, 1967. *ASHRAE Handbook of Fundamentals*, New York. American Society of Heating, Refrigerating, and Air-Conditioning Engineers, Inc.

ASHRAE, 1975. *ASHRAE Standard 51*, New York. American Society of Heating, Refrigerating, and Air-Conditioning Engineers, Inc.

ASHRAE, 2004, *Energy Consumption in Buildings Except Low-Rise Residential, Standard 90.1-2004*. Atlanta, GA. American Society of Heating, Refrigerating, and Air-Conditioning Engineers, Inc.

Chantrasrisalai, C and Fisher, D.E., Iu, I.S. and Eldridge, D.S., 2003. *Experimental Validation of Design Cooling Load Procedures: The Heat Balance Method*, *ASHRAE Transactions*, 109(2):160-173.

Eldridge, D.S. and Fisher, D.E., Chantrasrisalai, C, IU, I.S., 2003. *Experimental Validation of Design Cooling Load Procedures: Facility Construction*, *ASHRAE Transactions*, 109(2):151-159.

Fisher, D.E, 1995. *An Experimental Investigation of Mixed Convection Heat Transfer in a Rectangular Enclosure*. Ph.D. Thesis, University of Illinois, Urbana.

Fisher, D.E., and C.O. Pedersen. 1997. Convective Heat Transfer in Building Energy and Thermal Load Calculations, *ASHRAE Transactions*, vol. 103, pt. 2, pp. 137-148.

Incropera, F.P. and D.P. DeWitt, 1996. *Introduction to Heat Transfer*, 3rd Ed. Wiley, New York.

International Code Council, 2003. *International Energy Conservation Code*. Falls Church, VA.

Iu, I.S., D.E. Fisher, C. Chantrasrisalai, and D. Eldridge. 2003. Experimental Validation of Design Cooling Load Procedures: The Radiant Time Series Method, *ASHRAE Transactions*, 109(2):139-150.

Kline, S.J. and F.A. McClintock, 1953, Describing Uncertainties in single-sample experiments. *Mechanical Engineering* 57(1): 3-8.

McQuiston, F, and J.D. Spitler, 1992, *Cooling and Heating Load Calculation Manual*, Second Edition, ASHRAE

McQuiston, F. and J.D. Parker, and J.D. Spitler, 2000. *Heating, Ventilating, and Air Conditioning Analysis and Design*, Fifth Edition. John Wiley and Sons, New York.

Pedersen, C.O., D.E. Fisher, R.J. Liesen. 1997. Development of a Heat Balance Procedure for Calculating Cooling Loads, *ASHRAE Transactions*, Vol. 103, Pt. 2, pp. 459-468.

Pedersen, C.O, D.E. Fisher, J.D. Spitler, and R.J. Liesen, 1998, *Cooling and Heating Load Calculation Principles*. American Society of Heating, Refrigerating, and Air-Conditioning Engineers, Inc.

Pedersen, C.O., D.E. Fisher, R.J. Liesen, and R.K. Strand, 2001, ASHRAE Toolkit for building load calculations, *ASHRAE Transactions*.

Pedersen, C.O., 2001. *Building Loads Calculation Toolkit*, Atlanta, GA. American Society of Heating, Refrigerating, and Air-Conditioning Engineers, Inc.

Sherman, M.H, editor, *Air Change Rate and Airtightness in Buildings*, 1990, ASTM.

Spitler, J.D. 1996. *Annotated Guide to Load Calculation Models and Algorithms*, (Atlanta, Georgia: ASHRAE).

Spitler, J.D., D.E. Fisher, C.O. Pedersen. 1997. The Radiant Time Series Cooling Load Calculation Procedure, *ASHRAE Transactions*, Vol. 103, No. 2, pp. 503-515.

Spitler, J.D., and D.E. Fisher, 1999, On the relationship between the radiant time series and transfer function methods for design cooling load calculations. *International Journal of Heating, Ventilating, Air-Conditioning and Refrigerating Research* 5(2): 125-138. American Society of Heating, Refrigerating, and Air-Conditioning Engineers, Inc.

Walton, G.N., 1980. A New Algorithm for Radiant Interchange in Room Loads Calculations, *ASHRAE transactions*, Vol. 86, Part 2., pp. 190-208.

Walton, G.N., 1983. *Thermal Analysis Research Program Reference Manual*. National Bureau of Standards. NBSSIR 83-265.

Appendix A – RTSM and HBM ASHRAE Loads Toolkit

Input Files

This appendix shows the input files used in the study. The models contain RTSM inputs which are not used by the heat balance program.

!Builidng Name --> Heavy Building

!Builidng Construction --> Heavyweight

!Case --> Basecase

!Model --> HBM Tuned Model

!Time --> Sep 22, 2001

Date, 2001, 9, 22, TRUE;

SuccessiveSubstitutionData, 10, 8;

Location, Stillwater, 36.1, -97.1, -6, 300.0;

Environment, 98.87, 4.0, 180.0, 0.98, 0.0, 2, 0, 0, 0.2;

Zone, 3.05, 13.38, 0;

TempGround, 297.15;

Surface, SouthWall, WallConstruction, none, 180.0, 90.0, 4.70, 4.50, 0.7, 0.3, 0.90, 0.90, TOS, 3, 0, 0;

```
Surface, EastWall,    WallConstruction,  none,         90.0,  90.0, 11.15, 4.50,  0.7,  0.3, 0.90, 0.90, TOS, 3, 0, 0;
Surface, NorthWall,  WallConstruction,  none,          0.0,   90.0, 11.15, 4.50,  0.7,  0.3, 0.90, 0.90, TOS, 3, 0, 0;
Surface, WestWall,   WallConstruction,  none,      270.0,   90.0,  4.70,  4.50,  0.7,  0.3, 0.90, 0.90, TOS, 3, 0, 0;
Surface, Roof,        RoofConstruction,  none,           0.0,     0.0, 13.38, 6.10,  0.9,  0.3, 0.90, 0.90, TOS, 3, 0, 0;
Surface, Floor,       FloorConstruction, none,           0.0, 180.0, 13.38, 0.00, 0.5,  0.3, 0.90, 0.90,  TB, 3, 0, 0;
Surface, SouthWindow, SinglePaneWindow,  Clear3mm, 180.0,  90.0,  6.45, 4.50,  0.0,  0.0,  0.84,  0.84, TOS, 6, 2.54, 2.54;
Surface, WestWindow,  SinglePaneWindow,  Clear3mm, 270.0,  90.0,  6.45, 4.50,  0.0,  0.0,  0.84,  0.84, TOS, 6, 2.54, 2.54;

Window,Clear3mm,none,none,none,0.0,1.0,0.782,0.756,0.098,0.0,0.0,10,
! Angles
  0.0, 10.0, 20.0, 30.0, 40.0, 50.0, 60.0, 70.0, 80.0,90.0,
! SHGC
 0.860, 0.860, 0.858, 0.855, 0.846, 0.826, 0.779, 0.668, 0.418, 0.000,
! Absorptance, layer #1
 0.088, 0.089, 0.090, 0.093, 0.097, 0.101, 0.105, 0.108, 0.105, 0.000,
! Absorptance, layer #2
  0.0,  0.0,  0.0,  0.0,  0.0,  0.0,  0.0,  0.0,  0.0,  0.0,
! Absorptance, layer #3
  0.0,  0.0,  0.0,  0.0,  0.0,  0.0,  0.0,  0.0,  0.0,  0.0,
! Transmittance
 0.837, 0.836, 0.835, 0.830, 0.821, 0.800, 0.752, 0.639, 0.390, 0.000;
```

hout,SOUTHWALL , 8.6271496, 8.3750563, 9.0303898, 7.6470890, 7.2643371, 8.0324993, 8.6012506, 8.9931526, 9.3593388, 9.9389114, 11.0321522, 11.3499908, 11.7436972, 11.9939518, 12.8103409, 13.3476295, 13.2853394, 14.1214275, 13.1511459, 11.4699783, 10.6699438, 10.9881611, 11.8335590, 10.3909378;

hout,EASTWALL , 8.4736261, 8.2345676, 8.9224997, 7.5194192, 7.1383495, 7.9411097, 8.5295897, 9.2980032, 9.7551231, 10.2910519, 11.3423023, 11.5058060, 11.6163836, 11.5662374, 12.2752495, 12.7990685, 12.7548265, 13.7093182, 12.8318892, 11.1955051, 10.4244833, 10.7895803, 11.6791325, 10.1232977;

hout,NORTHWALL , 8.7388573, 8.5405359, 9.0846872, 7.9091301, 7.5257673, 8.2965393, 8.7716541, 9.0743818, 9.2996626, 9.6478662, 10.3162889, 10.3534260, 10.5643787, 10.6894550, 11.2418756, 11.6056137, 11.5898790, 12.2033386, 11.6980400, 10.6801548, 10.1673450, 10.4131689, 10.9810734, 10.0426292;

hout,WESTWALL , 8.9635363, 8.7432518, 9.2458601, 8.0852985, 7.6955423, 8.4254465, 8.8763714, 9.1596203, 9.3731747, 9.7540913, 10.3710241, 10.4135571, 10.5593185, 10.7404613, 11.5263138, 12.1233521, 12.3376131, 12.9500618, 12.3288250, 11.1380806, 10.5601330, 10.7337990, 11.8393450, 10.3959293;

hout,ROOF , 8.0858259, 7.8912349, 8.6466932, 7.2309766, 6.8494196, 7.7573733, 8.3829870, 8.7031879, 9.4638100, 10.3164854, 11.6459904, 12.6088333, 13.1403532, 13.3116436, 13.8563709, 14.0633850, 13.7318459, 14.1615210, 12.8388214, 10.8938637, 10.1372375, 10.5329237, 11.4691982, 10.0272293;

hout,FLOOR , 0.0000000;

hout,SOUTHWINDOW , 8.0613461, 7.8744984, 8.6000223, 7.2710938, 6.9469476, 7.7555065, 8.3519354, 8.7472277, 9.0646286, 9.5597153, 10.5286789, 10.5720167, 10.7566214, 10.8596039, 11.6291800, 12.1858292, 12.1584148, 13.1356049, 12.2488880, 10.6132841, 9.8784075, 10.2938957, 11.2324886, 9.8217106;

hout,WESTWINDOW , 8.4049616, 8.2500286, 8.8181410, 7.7112627, 7.3755898, 8.1459560, 8.6269264, 8.9263544, 9.1526365, 9.5404453, 10.1478539, 10.1800060, 10.3079014, 10.3891373, 10.9271173, 11.3026276, 11.3137665, 11.8651695, 11.3013878, 10.2408352, 9.7525425, 10.0231037, 11.2327271, 9.8219624;

!Radiative fraction

RadFrac,SOUTHWALL , 0.4249896;

RadFrac,EASTWALL , 0.4211849;

RadFrac,NORTHWALL , 0.4146830;

RadFrac,WESTWALL , 0.4248030;

RadFrac,ROOF , 0.4927195;

RadFrac,FLOOR , 0.4149342;

RadFrac,SOUTHWINDOW , 0.4035144;

RadFrac,WESTWINDOW , 0.4033571;

PRF,SOUTHWALL , 0.0171598, 0.0160434, 0.0185329, 0.0258568, 0.0342548, 0.0411071, 0.0457742, 0.0484325, 0.0494700, 0.0492763, 0.0481840, 0.0464598, 0.0443119, 0.0418995, 0.0393434, 0.0367333, 0.0341351, 0.0315962, 0.0291495, 0.0268170, 0.0246123, 0.0225428, 0.0206110, 0.0188163;

PRF,EASTWALL , 0.0146918, 0.0137060, 0.0174029, 0.0269405, 0.0372619, 0.0452563, 0.0503722, 0.0529858, 0.0536575, 0.0529047, 0.0511505, 0.0487248, 0.0458794, 0.0428025, 0.0396332, 0.0364719, 0.0333895, 0.0304345, 0.0276382, 0.0250188, 0.0225855, 0.0203403, 0.0182801, 0.0163986;

PRF,NORTHWALL , 0.0207175, 0.0068626, 0.0174270, 0.0353664, 0.0503536, 0.0595369, 0.0637641, 0.0644069, 0.0626256, 0.0592959, 0.0550550, 0.0503566, 0.0455171, 0.0407504, 0.0361957, 0.0319379, 0.0280228, 0.0244691, 0.0212766, 0.0184329, 0.0159177, 0.0137063, 0.0117720, 0.0100874;

PRF,WESTWALL , 0.0174025, 0.0162554, 0.0185692, 0.0255646, 0.0336642, 0.0403406, 0.0449532, 0.0476471, 0.0487774, 0.0487067, 0.0477482, 0.0461557, 0.0441294, 0.0418244, 0.0393592, 0.0368235, 0.0342839, 0.0317893, 0.0293742, 0.0270625, 0.0248694, 0.0228041, 0.0208705, 0.0190694;

PRF,ROOF , 0.0006143, 0.0066228, 0.0227989, 0.0344237, 0.0363820, 0.0339070, 0.0301360, 0.0262782, 0.0227331, 0.0196002, 0.0168749, 0.0145196, 0.0124898, 0.0107426, 0.0092393, 0.0079462, 0.0068341, 0.0058775, 0.0050549, 0.0043474, 0.0037389, 0.0032156, 0.0027655, 0.0023784;

PRF,FLOOR , 0.0002058, 0.0002061, 0.0002073, 0.0002083, 0.0002088, 0.0002090, 0.0002091, 0.0002090, 0.0002089, 0.0002087, 0.0002085, 0.0002083, 0.0002081, 0.0002079, 0.0002077, 0.0002075, 0.0002073, 0.0002071, 0.0002069, 0.0002068, 0.0002066, 0.0002064, 0.0002062, 0.0002060;

PRF,SOUTHWINDOW , 4.6517191, 0.0000000;

PRF,WESTWINDOW , 4.6517191, 0.0000000;

RTFnonsolar, 0.4452415, 0.0993168, 0.0599146, 0.0445291, 0.0365563, 0.0316758, 0.0282673, 0.0256443, 0.0234902, 0.0216476, 0.0200280, 0.0185794, 0.0172692, 0.0160724, 0.0149741, 0.0139620, 0.0130270, 0.0121587, 0.0113528, 0.0106037, 0.0099065, 0.0092574, 0.0086521, 0.0080880;

RTFsolar, 0.5803062, 0.1037854, 0.0633291, 0.0450467, 0.0333021, 0.0254670, 0.0201296, 0.0164156, 0.0137722, 0.0118413, 0.0103898, 0.0092639, 0.0083652, 0.0076248, 0.0070003, 0.0064604, 0.0059843, 0.0055593, 0.0051749, 0.0048234, 0.0045008, 0.0042031, 0.0039274, 0.0036712;

Construction, WallConstruction,Facebrick,Styrofoam,Hwconcrete;

Construction, RoofConstruction,Shingle,Tarpaper,Plywood,Styrofoam,Styrofoam,Plywood,Concrete,Metaldeck;

Construction,FloorConstruction,Metaldeck,Concrete;

Construction, SinglePaneWindow,glass;

MaterialLayer, Facebrick, 0.1016, 1.333, 2002.0, 0.92, 0.0, 0.0, 0.0, 0.0, 0.0, 0.0;

MaterialLayer, Hwconcrete, 0.2032, 1.731, 2243.0, 0.84, 0.0, 0.0, 0.0, 0.0, 0.0, 0.0;

MaterialLayer, Styrofoam, 0.0254, 0.028, 32.0, 1.21, 0.0, 0.0, 0.0, 0.0, 0.0, 0.0;

MaterialLayer, Plywood, 0.0127, 0.116, 540.0, 1.21, 0.0, 0.0, 0.0, 0.0, 0.0, 0.0;

MaterialLayer, Gypsum, 0.0127, 0.727, 1602.0, 0.84, 0.0, 0.0, 0.0, 0.0, 0.0, 0.0;

MaterialLayer, Shingle, 0.001, 0.0369, 1100.0, 1.51, 0.0, 0.0, 0.0, 0.0, 0.0, 0.0;

MaterialLayer, Tarpaper, 0.001, 0.0129, 1100.0, 1.26, 0.0, 0.0, 0.0, 0.0, 0.0, 0.0;

MaterialLayer, Metaldeck, 0.002, 45.0, 7689.0, 0.42, 0.0, 0.0, 0.0, 0.0, 0.0, 0.0;

MaterialLayer, Concrete, 0.1270, 0.1730, 641.0, 0.84, 0.0, 0.0, 0.0, 0.0, 0.0, 0.0;

MaterialLayer, glass, 0.0, 0.0, 0.0, 0.0, 0.00667, 0.0, 0.0, 0.0, 0.0, 0.0;

MaterialLayer, Fiberglass, 0.0889, 0.036, 96.0, 0.96, 0.0, 0.0, 0.0, 0.0, 0.0, 0.0;

MaterialLayer, Airspace, 0.0, 0.0, 0.0, 0.0, 0.176, 0.0, 0.0, 0.0, 0.0, 0.0;

MaterialLayer, AcousticTile, 0.019, 0.061, 481.00, 0.841, 0.0, 0.0, 0.0, 0.0, 0.0, 0.0;

PeopleSplits,0.58,0.42,0.33,0.67,130.0;

People,0.0,0.0,0.0,0.0,0.0,0.0,0.0,0.0,0.0,0.0,0.0,0.0,0.0,0.0,0.0,0.0,0.0,0.0,0.0,0.0,0.0,0.0,0.0,0.0;

EquipmentSplits,1.0,0.0,0.3,0.7;

Equipment,0.0,0.0,0.0,0.0,0.0,0.0,0.0,0.0,0.0,0.0,0.0,0.0,0.0,0.0,0.0,0.0,0.0,0.0,0.0,0.0,0.0,0.0,0.0,0.0;

LightingSplits,1.0,0.0,0.2,0.3,0.5,0.2;

Lighting,0.0,0.0,0.0,0.0,0.0,0.0,0.0,0.0,0.0,0.0,0.0,0.0,0.0,0.0,0.0,0.0,0.0,0.0,0.0,0.0,0.0,0.0,0.0,0.0;

SolarDist,SouthWall, 0.046104,SouthWindow, 0.063271,EastWall, 0.109375,NorthWall, 0.109375,WestWall, 0.046104,WestWindow, 0.063271,Roof, 0.13125,Floor,0.43125;

LWRadDist,SouthWall, 0.065863,SouthWindow, 0.090387,EastWall, 0.15625,NorthWall, 0.15625,WestWall, 0.065863,WestWindow, 0.090387,Roof, 0.1875,Floor, 0.1875;

SWRadDist,SouthWall, 0.065863,SouthWindow, 0.090387,EastWall, 0.15625,NorthWall, 0.15625,WestWall, 0.065863,WestWindow, 0.090387,Roof, 0.1875,Floor, 0.1875;

InfiltrationACH,0.25,0.25,0.25,0.25,0.25,0.25,0.25,0.25,0.25,0.25,0.25,0.25,0.25,0.25,0.25,0.25,0.25,0.25,0.25,0.25,0.25,0.25,0.25,0.25,0.25,0.25,0.25;

InfiltrationCoeffs,0.606,0.036,0.1177,0.0; ! These are BLAST defaults for metric units

Ventilation,0.0,0.0,0.0,0.0,0.0,0.0,0.0,0.0,0.0,0.0,0.0,0.0,0.0,0.0,0.0,0.0,0.0,0.0,0.0,0.0,0.0,0.0,0.0,0.0,0.0,0.0,0.0,0.0,0.0,0.0,0.0,0.0,0.0,0.0,0.0,0.0,0.0,0.0,0.0;

! Measured Input Data on Sep 22

! Outside Conditions

WindSpeed, 1.24, 1.14, 1.54, 0.80, 0.60, 1.08, 1.41, 1.62, 1.78, 2.03, 2.53, 2.49, 2.55, 2.58, 2.98, 3.28, 3.27, 3.83, 3.39, 2.55, 2.17, 2.40, 2.91, 2.16;

WindDirection, 122.50, 122.17, 100.58, 113.58, 132.50, 115.42, 106.08, 151.75, 157.00, 192.92, 138.42, 121.58, 127.08, 129.17, 117.42, 129.17, 121.92, 119.83, 125.33, 118.00, 119.92, 143.17, 170.92, 211.42;

SolarRadiation, 0.00, 0.00, 0.00, 0.00, 0.00, 0.00, 0.00, 38.00, 112.50, 202.50, 337.92, 699.25, 781.33, 774.33, 704.58, 571.67, 436.17, 228.92, 56.25, 0.00, 0.00, 0.00, 0.00, 0.00;

TempDewPoint, 291.33, 290.90, 290.61, 290.42, 289.89, 290.30, 290.34, 290.78, 291.30, 292.24, 292.84, 293.59, 294.32, 294.98, 295.53, 295.25, 295.01, 294.87, 294.56, 294.16, 293.83, 293.49, 292.90, 292.30;

TempOutside, 291.80, 291.37, 291.08, 290.74, 290.20, 290.60, 290.64, 291.08, 291.60, 292.53, 293.73, 296.38, 298.73, 300.31, 301.69, 302.24, 302.41, 301.82, 300.41, 297.87, 296.77, 295.96, 295.63, 294.94;

TempWetOutside, 291.49, 291.06, 290.77, 290.53, 290.00, 290.40, 290.44, 290.88, 291.40, 292.33, 293.12, 294.41, 295.57, 296.45, 297.19, 297.14, 297.02, 296.77, 296.19, 295.22, 294.69, 294.22, 293.72, 293.11;

TempSpecial, 300.57, 300.58, 300.57, 300.57, 300.58, 300.59, 300.61, 300.59, 300.59, 300.61, 300.58, 300.54, 300.54, 300.89, 300.63, 300.56, 300.54, 300.51, 300.30, 300.34, 300.56, 300.56, 300.56, 300.56;

! HeavyBldg Inside Conditions

TempInside, 300.57, 300.58, 300.57, 300.57, 300.58, 300.59, 300.61, 300.59, 300.59, 300.61, 300.58, 300.54, 300.54, 300.89, 300.63, 300.56, 300.54, 300.51, 300.30, 300.34, 300.56, 300.56, 300.56, 300.56;

TempDeck, 300.81, 301.04, 301.18, 301.40, 301.58, 301.77, 301.93, 301.73, 301.14, 300.49, 299.18, 296.81, 295.71, 295.31, 292.92, 291.72, 291.78, 293.05, 295.20, 297.89, 298.99, 299.49, 299.89, 300.21;

SystemAirForConvectionCalc, 20.94, 20.93, 20.91, 20.93, 20.92, 20.94, 20.90, 20.90, 20.91, 20.90, 20.91, 20.93, 20.92, 20.91, 20.85, 20.82, 20.83, 20.88, 20.96, 20.92, 20.93, 20.93, 20.93, 20.94;

!Builidng Name --> Light Building

!Builidng Construction --> Lightweight

!Case --> Basecase

!Model --> HBM Tuned Model

!Time --> Sep 22, 2001

Date, 2001, 9, 22, TRUE;

SuccessiveSubstitutionData, 10, 8;

Location, Stillwater, 36.1, -97.1, -6, 300.0;

Environment, 98.87, 4.0, 180.0, 0.98, 0.0, 2, 0, 0, 0.2;

Zone, 3.05, 13.38, 0;

TempGround, 297.15;

```
Surface, SouthWall,  WallConstruction,  none,       180.0,  90.0,  4.70,  4.50,  0.6,  0.3, 0.90, 0.90, TOS, 3, 0, 0;
Surface, EastWall,    WallConstruction,  none,        90.0,  90.0, 11.15, 4.50,  0.6,  0.3, 0.90, 0.90, TOS, 3, 0, 0;
Surface, NorthWall,  WallConstruction,  none,         0.0,   90.0, 11.15, 4.50,  0.6,  0.3, 0.90, 0.90, TOS, 3, 0, 0;
Surface, WestWall,   WallConstruction,  none,     270.0,   90.0,  4.70,  4.50,  0.6,  0.3, 0.90, 0.90, TOS, 3, 0, 0;
Surface, Roof,        RoofConstruction,  none,          0.0,     0.0, 13.38, 6.10,  0.9,  0.3, 0.90, 0.90, TOS, 3, 0, 0;
Surface, Floor,       FloorConstruction, none,          0.0, 180.0, 13.38, 0.00, 0.5,  0.3, 0.90, 0.90,  TB, 3, 0, 0;
Surface, SouthWindow, SinglePaneWindow,  Clear3mm, 180.0,  90.0,  6.45, 4.50,  0.0,  0.0,  0.84,  0.84, TOS, 6, 2.54, 2.54;
Surface, WestWindow,  SinglePaneWindow,  Clear3mm, 270.0,  90.0,  6.45, 4.50,  0.0,  0.0,  0.84,  0.84, TOS, 6, 2.54, 2.54;

Window,Clear3mm,none,none,none,0.0,1.0,0.782,0.756,0.098,0.0,0.0,10,
! Angles
  0.0, 10.0, 20.0, 30.0, 40.0, 50.0, 60.0, 70.0, 80.0,90.0,
! SHGC
 0.860, 0.860, 0.858, 0.855, 0.846, 0.826, 0.779, 0.668, 0.418, 0.000,
! Absorptance, layer #1
 0.088, 0.089, 0.090, 0.093, 0.097, 0.101, 0.105, 0.108, 0.105, 0.000,
! Absorptance, layer #2
  0.0,  0.0,  0.0,  0.0,  0.0,  0.0,  0.0,  0.0,  0.0,  0.0,
! Absorptance, layer #3
  0.0,  0.0,  0.0,  0.0,  0.0,  0.0,  0.0,  0.0,  0.0,  0.0,
! Transmittance
 0.837, 0.836, 0.835, 0.830, 0.821, 0.800, 0.752, 0.639, 0.390, 0.000;
```

hout,SOUTHWALL , 8.0180950, 7.7692461, 8.5771561, 7.0780163, 6.6455760, 7.6602688, 8.3173161, 8.7380753, 9.3212776, 10.0518017, 11.2590446, 11.8667755, 12.3011751, 12.4753246, 13.1265030, 13.4821682, 13.2785950, 13.9325504, 12.7993574, 10.9737158, 10.1221561, 10.4856596, 11.4496498, 9.9889288;

hout,EASTWALL , 8.0036936, 7.7766271, 8.5799160, 7.0820155, 6.6496243, 7.6616192, 8.3180323, 9.6136932, 10.1228819, 10.6130619, 11.5954895, 11.8591309, 11.7836189, 11.5005207, 12.1802578, 12.7027111, 12.6554489, 13.5833683, 12.6439304, 10.9045286, 10.0926495, 10.5015202, 11.4537678, 9.8712254;

hout,NORTHWALL , 8.3781414, 8.1953297, 8.8138247, 7.5939913, 7.1796370, 8.0916843, 8.6127968, 8.8974648, 9.2020531, 9.6273174, 10.3751574, 10.5827274, 10.8229542, 10.9572754, 11.4759369, 11.8088341, 11.7744827, 12.2805023, 11.6686058, 10.5203390, 9.9677086, 10.2265310, 10.8293180, 9.8723049;

hout,WESTWALL , 8.4017487, 8.1838522, 8.8091593, 7.5884409, 7.1743155, 8.0896530, 8.6115980, 8.9079094, 9.1958084, 9.6686888, 10.3755836, 10.5832729, 10.8235664, 11.0506859, 11.9735451, 12.6165295, 12.8238335, 13.2278233, 12.2943096, 10.7319393, 10.0462084, 10.2305489, 11.4455853, 9.9853973;

hout,ROOF , 8.0935955, 7.8981433, 8.6502924, 7.2384691, 6.8575702, 7.7606468, 8.3846130, 8.7090216, 9.4627972, 10.3170166, 11.6476440, 12.6117582, 13.1451244, 13.3175850, 13.8621082, 14.0684032, 13.7359791, 14.1640663, 12.8389111, 10.8965931, 10.1397400, 10.5346889, 11.4697132, 10.0293522;

hout,FLOOR , 0.0000000;

hout,SOUTHWINDOW , 8.0396719, 7.8550224, 8.5835619, 7.2526836, 6.9289579, 7.7415209, 8.3399315, 8.7400818, 9.0572128, 9.5552845, 10.5321140, 10.5869436, 10.7809048, 10.8856735, 11.6606073, 12.2214203, 12.1909647, 13.1587620, 12.2626343, 10.5905361, 9.8635368, 10.2788305, 11.2203579, 9.8087921;

hout,WESTWINDOW , 8.3845129, 8.2318382, 8.8021002, 7.6946683, 7.3595781, 8.1329422, 8.6153603, 8.9192629, 9.1449871, 9.5355530, 10.1511345, 10.1958447, 10.3355389, 10.4200783, 10.9636612, 11.3419991, 11.3472633, 11.8889961, 11.3150024, 10.2163715, 9.7369328, 10.0070667, 11.2203140, 9.8087502;

!Radiative fraction

RadFrac,SOUTHWALL , 0.4369113;

RadFrac,EASTWALL , 0.4332002;

RadFrac,NORTHWALL , 0.4268192;

RadFrac,WESTWALL , 0.4368743;

RadFrac,ROOF , 0.4995900;

RadFrac,FLOOR , 0.4267613;

RadFrac,SOUTHWINDOW , 0.4153012;

RadFrac,WESTWINDOW , 0.4151293;

PRF,SOUTHWALL , 0.0029345, 0.0425455, 0.0688400, 0.0542074, 0.0371016, 0.0247333, 0.0164020, 0.0108655, 0.0071963, 0.0047659, 0.0031563, 0.0020903, 0.0013844, 0.0009168, 0.0006072, 0.0004021, 0.0002663, 0.0001764, 0.0001168, 0.0000774, 0.0000512, 0.0000339, 0.0000225, 0.0000149;

PRF,EASTWALL , 0.0028952, 0.0422396, 0.0687065, 0.0542360, 0.0371587, 0.0247885, 0.0164488, 0.0109031, 0.0072256, 0.0047882, 0.0031730, 0.0021027, 0.0013934, 0.0009233, 0.0006119, 0.0004055, 0.0002687, 0.0001781, 0.0001180, 0.0000782, 0.0000518, 0.0000343, 0.0000228, 0.0000151;

PRF,NORTHWALL , 0.0027567, 0.0409686, 0.0681104, 0.0543380, 0.0373923, 0.0250177, 0.0166447, 0.0110615, 0.0073494, 0.0048828, 0.0032440, 0.0021552, 0.0014319, 0.0009513, 0.0006320, 0.0004199, 0.0002790, 0.0001853, 0.0001231, 0.0000818, 0.0000544, 0.0000361, 0.0000240, 0.0000159;

PRF,WESTWALL , 0.0028527, 0.0419159, 0.0685614, 0.0542655, 0.0372197, 0.0248475, 0.0164990, 0.0109435, 0.0072571, 0.0048122, 0.0031910, 0.0021160, 0.0014031, 0.0009304, 0.0006169, 0.0004091, 0.0002713, 0.0001799, 0.0001193, 0.0000791, 0.0000524, 0.0000348, 0.0000231, 0.0000153;

PRF,ROOF , 0.0577350, 0.1991191, 0.0986358, 0.0387232, 0.0151843, 0.0059541, 0.0023347, 0.0009155, 0.0003590, 0.0001408, 0.0000552, 0.0000216, 0.0000085, 0.0000033, 0.0000013, 0.0000005, 0.0000002, 0.0000001, 0.0000000, 0.0000000, 0.0000000, 0.0000000, 0.0000000, 0.0000000;

PRF,FLOOR , 0.0002051, 0.0002071, 0.0002094, 0.0002102, 0.0002102, 0.0002101, 0.0002098, 0.0002096, 0.0002093, 0.0002090, 0.0002087, 0.0002085, 0.0002082, 0.0002079, 0.0002076, 0.0002074, 0.0002071, 0.0002068, 0.0002065, 0.0002063, 0.0002060, 0.0002057, 0.0002054, 0.0002052;

PRF,SOUTHWINDOW , 4.5179300, 0.0000000;

PRF,WESTWINDOW , 4.3581209, 0.0000000;

RTFnonsolar, 0.6394221, 0.1887818, 0.0842988, 0.0403380, 0.0204476, 0.0109375, 0.0061398, 0.0035932, 0.0021755, 0.0013533, 0.0008590, 0.0005541, 0.0003614, 0.0002378, 0.0001577, 0.0001038, 0.0000700, 0.0000469, 0.0000299, 0.0000201, 0.0000127, 0.0000087, 0.0000059, 0.0000038;

RTFsolar, 0.6258617, 0.1783921, 0.0916269, 0.0481020, 0.0254225, 0.0135759, 0.0073517, 0.0040513, 0.0022781, 0.0013093, 0.0007699, 0.0004624, 0.0002837, 0.0001779, 0.0001123, 0.0000712, 0.0000461, 0.0000294, 0.0000186, 0.0000120, 0.0000080, 0.0000055, 0.0000035, 0.0000026;

Construction, WallConstruction,Stucco,Styrofoam,Plywood,Fiberglass,Gypsum;

Construction, RoofConstruction,Shingle,Tarpaper,Plywood,Styrofoam,Styrofoam,Plywood,Airspace,Metaldeck;

Construction,FloorConstruction,Metaldeck,Concrete;

Construction, SinglePaneWindow,glass;

MaterialLayer, Stucco, 0.0064, 0.692, 1858.0, 0.84, 0.0, 0.0, 0.0, 0.0, 0.0, 0.0;

MaterialLayer, Styrofoam, 0.0254, 0.028, 32.0, 1.21, 0.0, 0.0, 0.0, 0.0, 0.0, 0.0;

MaterialLayer, Plywood, 0.0127, 0.116, 540.0, 1.21, 0.0, 0.0, 0.0, 0.0, 0.0, 0.0;

```
MaterialLayer, Fiberglass, 0.0889, 0.036,  96.0,   0.96,    0.0, 0.0, 0.0, 0.0, 0.0, 0.0;
MaterialLayer, Gypsum,     0.0127, 0.727,  1602.0, 0.84,    0.0, 0.0, 0.0, 0.0, 0.0, 0.0;
MaterialLayer, Shingle,    0.001,  0.0369, 1100.0, 1.51,    0.0, 0.0, 0.0, 0.0, 0.0, 0.0;
MaterialLayer, Tarpaper,   0.001,  0.0129, 1100.0, 1.26,    0.0, 0.0, 0.0, 0.0, 0.0, 0.0;
MaterialLayer, Metaldeck,  0.002,  45.0,   7689.0, 0.42,    0.0, 0.0, 0.0, 0.0, 0.0, 0.0;
MaterialLayer, Concrete,   0.0889, 0.1730,  641.0, 0.84,    0.0, 0.0, 0.0, 0.0, 0.0, 0.0;
MaterialLayer, glass,       0.0,   0.0,      0.0,  0.0, 0.00667, 0.0, 0.0, 0.0, 0.0, 0.0;
MaterialLayer, Airspace,    0.0,   0.0,      0.0,  0.0,  0.176, 0.0, 0.0, 0.0, 0.0, 0.0;
MaterialLayer, AcousticTile, 0.019,  0.061,  481.00, 0.841, 0.0,   0.0, 0.0, 0.0, 0.0, 0.0;

PeopleSplits,0.58,0.42,0.33,0.67,130.0;
People,0.0,0.0,0.0,0.0,0.0,0.0,0.0,0.0,0.0,0.0,0.0,0.0,0.0,0.0,0.0,0.0,0.0,0.0,0.0,0.0,0.0,0.0,0.0,0.0;

EquipmentSplits,1.0,0.0,0.3,0.7;
Equipment,0.0,0.0,0.0,0.0,0.0,0.0,0.0,0.0,0.0,0.0,0.0,0.0,0.0,0.0,0.0,0.0,0.0,0.0,0.0,0.0,0.0,0.0,0.0,0.0;

LightingSplits,1.0,0.0,0.2,0.3,0.5,0.2;
Lighting,0.0,0.0,0.0,0.0,0.0,0.0,0.0,0.0,0.0,0.0,0.0,0.0,0.0,0.0,0.0,0.0,0.0,0.0,0.0,0.0,0.0,0.0,0.0,0.0;

SolarDist,SouthWall,  0.046104,SouthWindow,  0.063271,EastWall,  0.109375,NorthWall,  0.109375,WestWall,  0.046104,WestWindow,  0.063271,Roof, 0.13125,Floor,0.43125;
LWRadDist,SouthWall, 0.065863,SouthWindow,  0.090387,EastWall, 0.15625,NorthWall, 0.15625,WestWall, 0.065863,WestWindow,  0.090387,Roof, 0.1875,Floor, 0.1875;
SWRadDist,SouthWall, 0.065863,SouthWindow,  0.090387,EastWall, 0.15625,NorthWall, 0.15625,WestWall, 0.065863,WestWindow,  0.090387,Roof, 0.1875,Floor, 0.1875;
```

InfiltrationACH,0.25,0.25,0.25,0.25,0.25,0.25,0.25,0.25,0.25,0.25,0.25,0.25,0.25,0.25,0.25,0.25,0.25,0.25,0.25,0.25,0.25,0.25,0.25,0.25,0.25,0.25,0.25,0.25,0.25;

InfiltrationCoeffs,0.606,0.036,0.1177,0.0; ! These are BLAST defaults for metric units

Ventilation,0.0,0.0,0.0,0.0,0.0,0.0,0.0,0.0,0.0,0.0,0.0,0.0,0.0,0.0,0.0,0.0,0.0,0.0,0.0,0.0,0.0,0.0,0.0,0.0,0.0,0.0,0.0,0.0,0.0,0.0,0.0,0.0,0.0;

! Measured Input Data on Sep 22

! Outside Conditions

WindSpeed, 1.24, 1.14, 1.54, 0.80, 0.60, 1.08, 1.41, 1.62, 1.78, 2.03, 2.53, 2.49, 2.55, 2.58, 2.98, 3.28, 3.27, 3.83, 3.39, 2.55, 2.17, 2.40, 2.91, 2.16;

WindDirection, 122.50, 122.17, 100.58, 113.58, 132.50, 115.42, 106.08, 151.75, 157.00, 192.92, 138.42, 121.58, 127.08, 129.17, 117.42, 129.17, 121.92, 119.83, 125.33, 118.00, 119.92, 143.17, 170.92, 211.42;

SolarRadiation, 0.00, 0.00, 0.00, 0.00, 0.00, 0.00, 0.00, 38.00, 112.50, 202.50, 337.92, 699.25, 781.33, 774.33, 704.58, 571.67, 436.17, 228.92, 56.25, 0.00, 0.00, 0.00, 0.00, 0.00;

TempDewPoint, 291.33, 290.90, 290.61, 290.42, 289.89, 290.30, 290.34, 290.78, 291.30, 292.24, 292.84, 293.59, 294.32, 294.98, 295.53, 295.25, 295.01, 294.87, 294.56, 294.16, 293.83, 293.49, 292.90, 292.30;

TempOutside, 291.80, 291.37, 291.08, 290.74, 290.20, 290.60, 290.64, 291.08, 291.60, 292.53, 293.73, 296.38, 298.73, 300.31, 301.69, 302.24, 302.41, 301.82, 300.41, 297.87, 296.77, 295.96, 295.63, 294.94;

TempWetOutside, 291.49, 291.06, 290.77, 290.53, 290.00, 290.40, 290.44, 290.88, 291.40, 292.33, 293.12, 294.41, 295.57, 296.45, 297.19, 297.14, 297.02, 296.77, 296.19, 295.22, 294.69, 294.22, 293.72, 293.11;

TempSpecial, 300.57, 300.67, 300.65, 300.73, 300.76, 300.75, 300.75, 300.81, 300.66, 300.61, 300.68, 300.63, 300.62, 300.78, 300.65, 300.74, 300.57, 300.56, 300.48, 299.80, 300.61, 300.61, 300.67, 300.71;

! LightBldg Inside Conditions

TempInside, 300.57, 300.67, 300.65, 300.73, 300.76, 300.75, 300.75, 300.81, 300.66, 300.61, 300.68, 300.63, 300.62, 300.78, 300.65, 300.74, 300.57, 300.56, 300.48, 299.80, 300.61, 300.61, 300.67, 300.71;

TempDeck, 302.64, 303.13, 303.45, 303.73, 303.92, 304.10, 304.16, 303.80, 302.47, 301.46, 300.01, 296.63, 294.17, 292.80, 290.19, 288.60, 288.07, 289.62, 292.74, 296.54, 300.14, 300.81, 301.57, 302.19;

SystemAirForConvectionCalc, 19.03, 19.04, 19.06, 19.02, 19.02, 19.03, 19.01, 19.00, 19.04, 19.04, 19.03, 19.03, 19.05, 19.06, 18.97, 18.94, 18.91, 18.97, 19.00, 19.04, 19.01, 19.02, 19.01, 19.00;

VITA

David S. Eldridge, Jr

Candidate for the Degree of

Master of Science

Thesis: DESIGN OF AN EXPERIMENTAL FACILITY FOR THE VALIDATION OF COOLING LOAD CALCULATION PROCEDURES

Major Field: Mechanical Engineering

Biographical:

Personal Data:

Grew up on a farm in Western Illinois, attended Westmer High School and University of Illinois, Urbana-Champaign prior to graduate school at Oklahoma State University. Currently working as a project engineer at a Chicago-area consulting firm specializing in energy efficiency and sustainable services.

Education:

BSME University of Illinois, Urbana-Champaign

Completed the Requirements for the Master of Science degree at Oklahoma State University in (May, 2007)

Experience:

Project Engineer at Grumman/Butkus Associates

Professional Memberships:

ASHRAE, USGBC

Name: David S. Eldridge, Jr. Date of Degree: May, 2007

Institution: Oklahoma State University Location: Stillwater, Oklahoma

Title of Study: DESIGN OF AN EXPERIMENTAL FACILITY FOR THE VALIDATION OF COOLING LOAD CALCULATION PROCEDURES

Pages in Study: 119 Candidate for the Degree of Master of Science

Major Field: Mechanical Engineering

Scope and Method of Study:

Two test cells were constructed to validate the ASHRAE cooling load calculation procedures developed under RP-875 and codified in the ASHRAE Loads Toolkit (RP987). The test cells were designed to test the cooling load procedures' ability to accurately predict cooling loads dominated by solar and transient conduction heat gains. Internal heat sources were eliminated and infiltration was minimized for the study. The construction of the test cells also examined the procedures' ability to differentiate between thermal mass effects.

Findings and Conclusions:

Laboratory and field testing validated the design and control of the facility prior to data collection. Preliminary tests showed that the facility was capable of validating the new ASHRAE cooling load procedures. The experimental uncertainty associated with the measured cooling load was less than 7.5% and model input parameters were well defined for baseline configurations.

ADVISER'S APPROVAL: Daniel E. Fisher, P.E.